Scientific and Validation Report for the Precipitation Product Processors of the NWC/GEO

NWC/CDOP3/GEO/AEMET/SCI/VR/Precipitation, Issue 1, Rev. 1
18 December 2019

Applicable to

GEO-PC-v154 (NWC-019)
GEO-CRR-v402 (NWC-024)
GEO-PC-Ph-v2.0 (NWC-077)
GEO-CRR-Ph-v2.0 (NWC-081)

Prepared by AEMET

REPORT SIGNATURE TABLE

Function	Name	Signature	Date
Prepared by	José Alberto Lahuerta (AEMET)		*18 December 2019*
Reviewed by	Xavier Calbet (AEMET) Pilar Rípodas (AEMET)		*18 December 2019*
Authorised by	Pilar Rípodas NWC SAF Project Manager		*18 December 2019*

DOCUMENT CHANGE RECORD

Version	Date	Pages	CHANGE(S)
1.0	21 January 2019	61	First version of precipitation products validation for NWC SAF SW Package GEO v2018 DRR. Content derived from Scientific and Validation Report for the Precipitation Product Processors of the NWC/GEO v2016 NWC/CDOP2/GEO/AEMET/VR/Precipitation
1.1	18 December 2019	65	Updated with GOES-16 section

LIST OF TABLES AND FIGURES

1. INTRODUCTION

The EUMETSAT "Satellite Application Facilities" (SAF) are dedicated centres of excellence for processing satellite data, and form an integral part of the distributed EUMETSAT Application Ground Segment (http://www.eumetsat.int). This documentation is provided by the SAF on Support to Nowcasting and Very Short Range Forecasting, NWC SAF. The main objective of NWC SAF is to provide, further develop and maintain software packages to be used for Nowcasting applications of operational meteorological satellite data by National Meteorological Services. More information can be found at the NWC SAF webpage, http://www.nwcsaf.org. This document is applicable to the NWC SAF processing package for geostationary meteorological satellites, NWC/GEO.

1.1 SCOPE OF THE DOCUMENT

This document is the Validation Report (VR) for the precipitation GEO products Precipitating Clouds (PC), Convective Rainfall Rate (CRR) and Precipitation products from Cloud Physical Properties (PPh) of the NWC/GEO software package. PPh generates two different products: Precipitating Clouds from Cloud Physical Properties (PC-Ph) and Convective Rainfall rate from Cloud Physical Properties (CRR-Ph).
This document compares the accuracies of the GEO precipitation products to the threshold accuracies for CDOP3 listed in the " NCWSAF product requirements document" *[AD. 4]*.

1.2 SOFTWARE VERSION IDENTIFICATION

This document applies to the algorithms implemented in the release 2018 of the NWC/GEO software package (GEO-PC-v1.5.4, GEO-CRR-v4.0.2, GEO-PC-Ph-v2.0 and GEO-CRR-Ph-v2.0).

1.3 IMPROVEMENT FROM PREVIOUS VERSIONS

Since 2016 release, these technical improvements have been implemented:

- Interface to updated NWCLIB
- New calibration of PPh products
- New PPh products validation with day/night distinction.

1.4 DEFINITIONS, ACRONYMS AND ABBREVIATIONS

AEMET	Agencia Estatal de Meteorología
ATBD	Algorithm Theoretical Basis Document
BALTRAD	Baltic Radar Network
CAPPI	Constant Altitude Plan Position Indicator
COT	Cloud Optical Thickness
CRR-Ph	Convective Rainfall Rate from Cloud Physical Properties
CRR	Convective Rainfall Rate
CSI	Critical Success Index
CT	Cloud Type
CWP	Cloud Water Path
NCAR EOL	Earth Observing Laboratory

ET	Echotop
EUMETSAT	European Organisation for the Exploitation of Meteorological Satellites
FAR	False Alarm Ratio
HRIT	High Rate Information Transmission
ICD	Interface Control Document
ICP	Illumination Conditions Parameter
IQF	Illumination Quality Flag
IR	Infrared
MAE	Mean Absolute Error
CTMP	Cloud Top Microphysical Properties
ME	Mean Error
MRV	Maximum Reflectivity in the Vertical
MSG	Meteosat Second Generation
NIR	Near Infrared
NWCLIB	Nowcasting SAF Library
NWC SAF	Satellite Application Facility for Nowcasting
PC	Precipitating Clouds
PC	Percentage of Corrects
PC-Ph	Precipitating Clouds from Cloud Physical Properties
PGE	Product Generation Element
POD	Probability of Detection
PoP	Probability of Precipitation
PPh	Precipitation from Cloud Physical Properties
PPI	Plan Position Indicator
PWRH	Moisture Correction Factor
R_{eff}	Effective Radius
RLR	Rainfall-Lightning Ratio
RMSE	Root Mean Square Error
RR	Rain Rate
SAF	Satellite Application Facility
SEVIRI	Spinning Enhanced Visible and Infrared Imager
SW	Software
USA	United States of America
2-V	2-Variable
3-V	3-Variable
VIS	Visible
VIS-N	Normalized Visible
WV	Water Vapour

1.5 REFERENCES

1.5.1 Applicable Documents

The following documents, of the exact issue shown, form part of this document to the extent specified herein. Applicable documents are those referenced in the Contract or approved by the Approval Authority. They are referenced in this document in the form [AD.X].

For dated references, subsequent amendments to, or revisions of, any of these publications do not apply. For undated references, the current edition of the document referred applies.
Current documentation can be found at the NWC SAF Helpdesk web: http://www.nwcsaf.org

Reference	Title	Code	Vers	Date
[AD. 1]	Proposal for the Third Continuous Development and Operations Phase (CDOP-3) March 2017 – February 2022	NWC SAF:CDOP-3 proposal	1.0	11/04/16
[AD. 2]	NWCSAF Project Plan	NWC/CDOP3/SAF/AEMET/MGT/PP	1.0	06/03/18
[AD. 3]	Configuration Management Plan for the NWC SAF	NWC/CDOP3/SAF/AEMET/MGT/CMP	1.0	21/02/18
[AD. 4]	NWCSAF Product Requirements Document	NWC/CDOP3/SAF/AEMET/MGT/PRD	1.0	31/01/18

Table 1. List of Applicable Documents

1.5.2 Reference Documents

The reference documents contain useful information related to the subject of the project. These reference documents complement the applicable ones, and can be looked up to enhance the information included in this document if it is desired. They are referenced in this document in the form [RD.X].
For dated references, subsequent amendments to, or revisions of, any of these publications do not apply. For undated references, the current edition of the document referred applies.
Current documentation can be found at the NWC SAF Helpdesk web: http://www.nwcsaf.org

Reference	Title	Code	Vers	Date
[RD 1]	Interface Control Document for Internal and External Interfaces of the NWC/GEO	NWC/CDOP3/GEO/AEMET/SW/ICD/1	1.0	21/01/19
[RD 2]	Data Output Format for the NWC/GEO	NWC/CDOP3/GEO/AEMET/SW/DOF	1.0	21/01/19
[RD 3]	Algorithm Theoretical Basis Document for SAFNWC/MSG "Precipitating Cloud" (PC-PGE04 v1.5)	SAF/NWC/CDOP2/SMHI/SCI/ATBD/4	1.5.4	15/07/13
[RD 4]	Algorithm Theoretical Basis Document for the Precipitation Product Processors of the NWC/GEO	NWC/CDOP2/GEO/AEMET/SCI/ATBD/Precipitation	2.1	21/01/19
[RD 5]	User Manual for the SAFNWC/MSG Parallax Correction Tool	GMV/SAFCDOP/VSAREP/02	1.0	02/06/08
[RD 6]	Adaptation of GEO PC-Ph product for MTG	NWC/CDOP3/MTG/AEMET/SCI/RP/PC-Ph	1.0	19/07/17

Table 2. List of Referenced Documents

2. VALIDATION FOR PRECIPITATING CLOUDS PRODUCT

This section contains the results obtained from the validation of the PC product which is described in the Algorithm Theoretical Basis Document for SAFNWC/MSG "Precipitating Cloud" (PC-PGE04 v1.5) [RD 3].

2.1 SUBJECTIVE VALIDATION FOR PRECIPITATING CLOUDS (PC)

Many cases have been visually studied by comparing the probability of precipitation (PoP) obtained from the PC algorithm against the radar data. Since PC product estimates probability of precipitation occurrence, the most suitable product to compare with would be the one that assigns 100% PoP where it is raining and 0% otherwise. So PC product has been compared with modified PPI product radar images where pixels with rain rates higher than or equal to 0.2 mm/h are set as rainy pixels (red colour) and the others as no rainy pixels (black colour).
A selection of cases that show the general behaviour of this product can be seen below. Since satellite scanning over the Iberian Peninsula takes place about 10 minutes later than the satellite imagery nominal time, PC images have been compared to radar ones taken 10 minutes later for a better time matching.

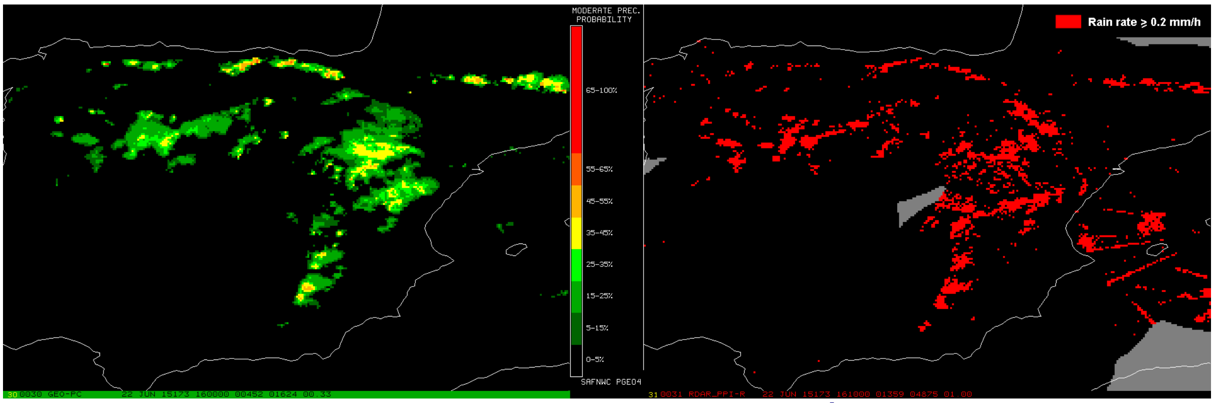

Figure 1. Comparison of PC product and radar (PPI) on 22nd June 2015 at 16:00UTC.

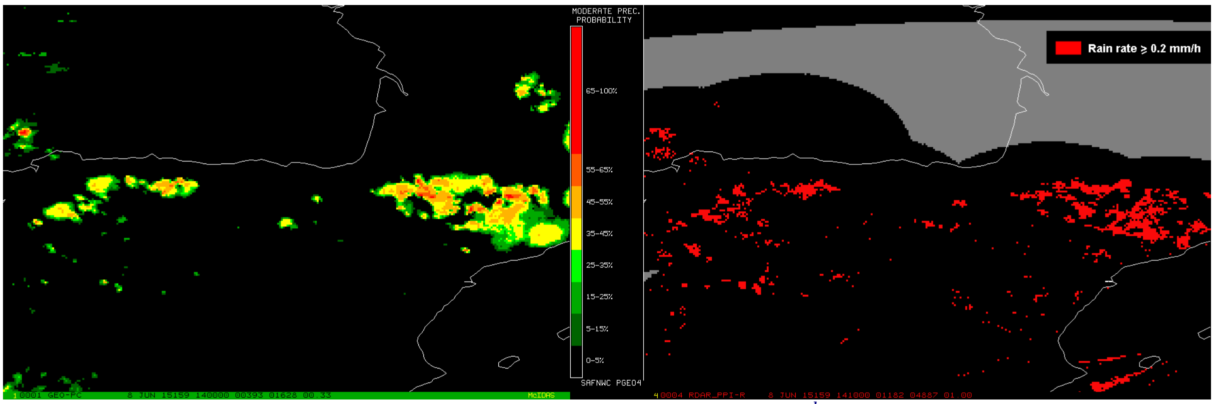

Figure 2. Comparison of PC product and radar (PPI) on 8th June 2015 at 14:00UTC.

Both Figure 1 and Figure 2 show day-time PC algorithm estimations where the overall precipitation areas are well depicted. However, PoP assigned are not so high, above all in the case of Figure 1, where few pixels take values of PoP higher than 50%. This fact could be explained by the time of the scanning of the satellite imagery used to compute the product. The set of satellite channels used by day-time PC algorithm includes some solar channels with valuable information for precipitation detection. The poorer are the illumination conditions, the lower is the confidence of the algorithm to assign higher PoPs.

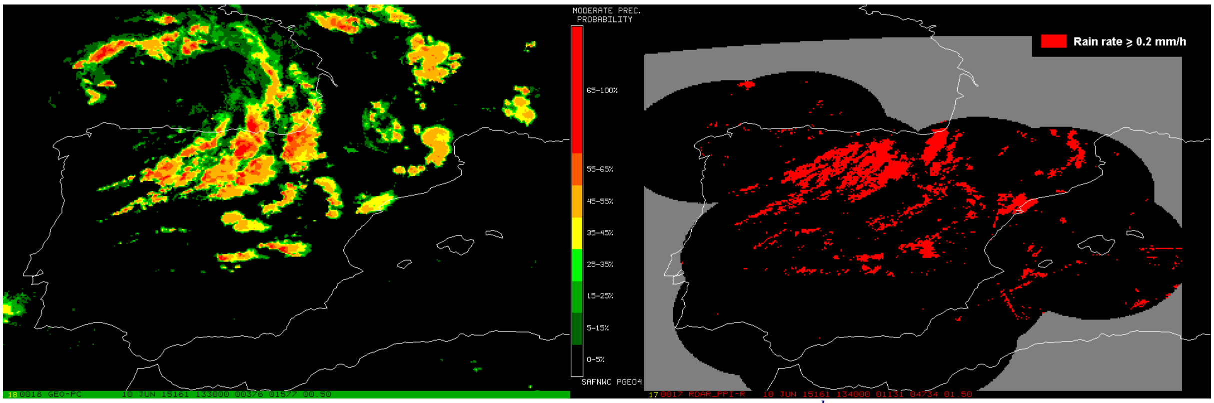

Figure 3. Comparison of PC product and radar (PPI) on 10th June 2015 at 13:30UTC.

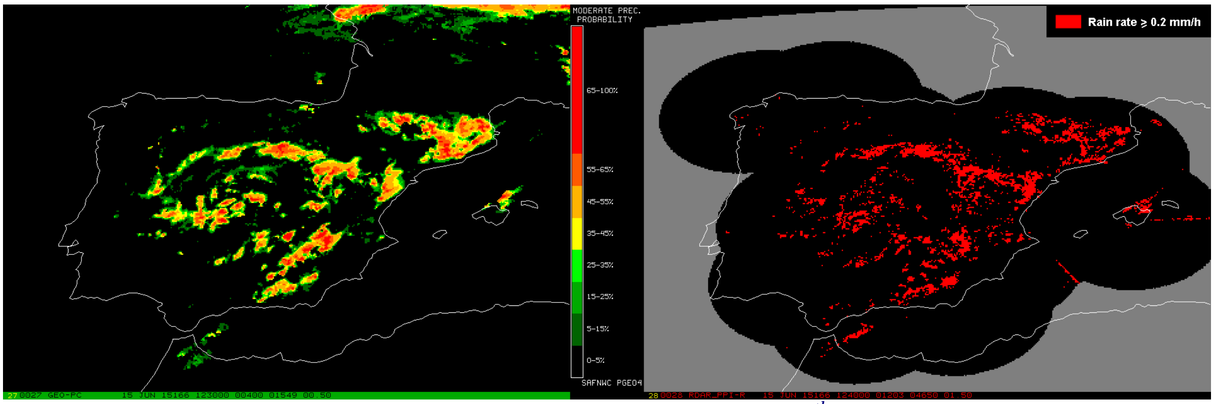

Figure 4. Comparison of PC product and radar (PPI) on 15th June 2015 at 12:30UTC.

Figure 3 and Figure 4 show day-time PC algorithm estimations with better illumination conditions than Figure 1 and Figure 2. In these cases it can be observed that the estimated precipitation areas are in good agreement with the radar ones and also that higher PoPs have been assigned.

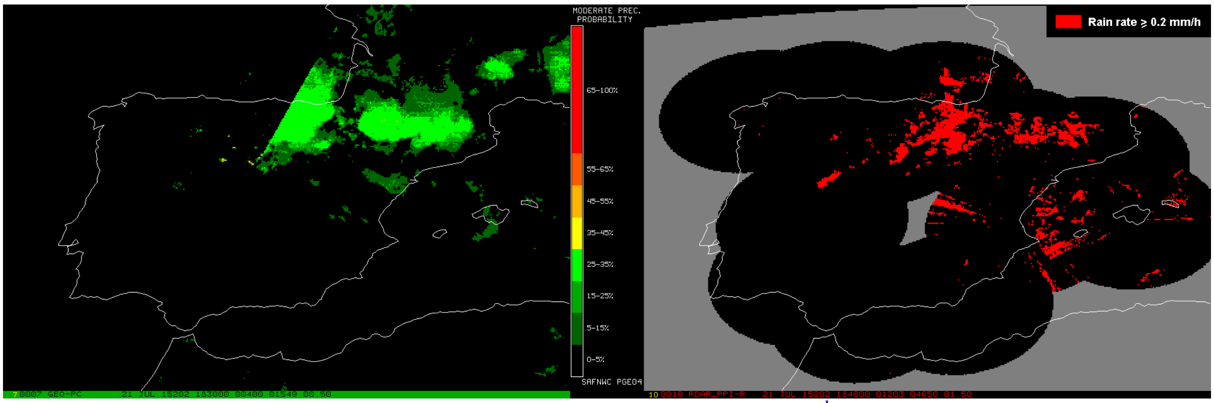

Figure 5. Comparison of PC product and radar (PPI) on 21th June 2015 at 18:30UTC

Figure 5 shows a scene with a day-night transition of PC algorithms. The day-time algorithm is displayed on the right side of the abrupt precipitation product transition. The night-time algorithm is displayed on the left side of this feature. At this time PC day-time algorithm is computed under poor illumination conditions, and so, there is a low confidence in the assignment of PoP. On the other hand night-time algorithm, which also shows a low confidence in the assignment of PoP, estimates bigger precipitation areas with more false alarms.

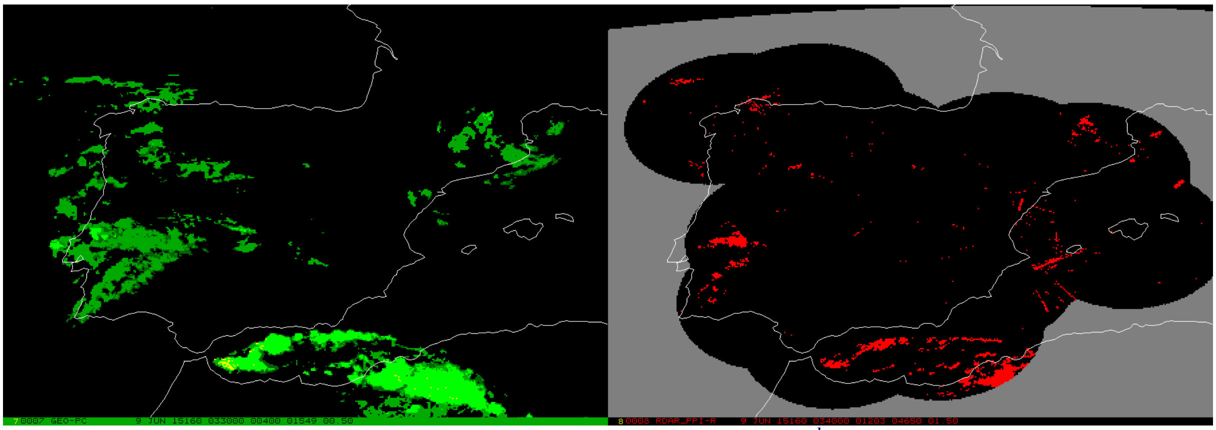

Figure 6. Comparison of PC product and radar (PPI) on 9th June 2015 at 03:30UTC

Figure 6 shows a night time scene where almost all precipitation areas depicted in the radar image are detected by PC product. However, since less information is contained in the night-time algorithm than in the day-time one, the confidence of PoP is lower. Also, the precipitation areas are overestimated providing a higher number of false alarms.

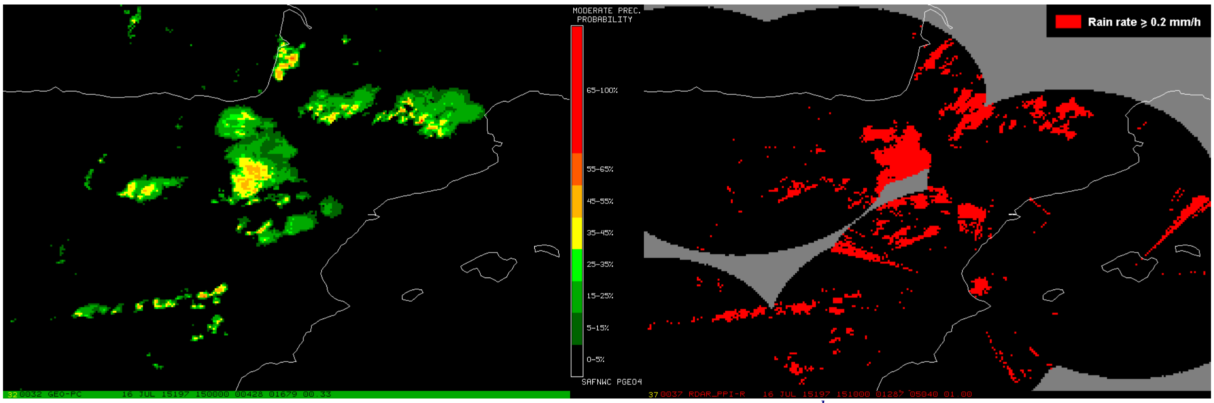

Figure 7. Comparison of PC product and radar (PPI) on 16th June 2015 at 15:00UTC.

Figure 7 shows a scene where there is a lack of several radars to compute a radar mosaic, and so there is no information over some areas. Here the usefulness of the PC product is shown. It is in agreement with the radar covered areas and complements its information over the rest of the image.

2.2 OBJECTIVE VALIDATION FOR PRECIPITATING CLOUDS (PC)

2.2.1 Validation Procedure

An objective validation for the PC algorithm against Spanish composite radar data has been done. The dataset used for this validation contains 103 rainy days throughout 2008.

Both day-time and night-time algorithms have been validated. Day-time algorithm has been used for those cases with sun zenith angles lower than 80º and night-time algorithm has been used for the rest of the cases.

The original radar data is in Lambert projection, for a better matching, it has been customary reprojected to the MSG projection using a bi-linear interpolation scheme. The NWCSAF parallax tool *[RD 5]* has been applied to the PC product. A comparison against radar data in 3x3 MSG pixels boxes in a yes/no way has been done. The horizontal resolution of the pixels are 3kms at satellite point .As detection of very light rain rates using GEO satellite data is not possible, the threshold to consider a radar pixel as rainy has been fixed at 0.2 mm/h.

Ground echoes in PPI scenes have been removed. To do that, a filter image, available as a radar product, has been used in order to remove ground echoes (wind mills,…). Ground echoes, like anomalous propagation echoes, have been removed through the 10.8IR scene. To do that, a rain image has been obtained from the 10.8IR data using the basic AUTOESTIMATOR algorithm (Vicente et al., 1998). A pixel with significant radar echo is considered to be a ground echo and set to zero if no significant value is found in a 15x15 centred box in the AUTOESTIMATOR image.

Although satellite data have been used for decluttering the radar data, since this information has been used in a non-aggressive way, datasets are still independent enough for statistical comparison in the validation.

In order to avoid a high number of correct negative comparisons that can contaminate the computation of validation scores, the validation area has been restricted to 15x15 pixel boxes around radar pixels with at least 0.2 mm/h. As some PC rainy pixels can appear out of the previous validation area, those pixels have been added to the final validation area in order to include all the possible false alarms.

Due to the temporal resolution of the SEVIRI data in the normal mode, there are four PC outputs available every hour. The Spanish radar network generates a set of instantaneous products every 10 minutes. The MSG scanning over Spain is done over 10 minutes after the time of the slot. The only way to match temporally PC and radar scenes is choosing 0 and 30 minutes PC images corresponding to 10 and 40 minutes radar images respectively. As 15 and 45 minutes PC images don't match temporally with the radar ones, those images haven't been used in the validation process.

A smoothing in 3x3 MSG pixels boxes has been applied in order to reduce the radar and satellite estimations spatial mismatching. One every three ordered pixels of the smoothed fields have been taken into account.

The verification metric computed for this validation is described in ANNEX 1: .

Since this is a yes/no validation only categorical scores have been computed.

2.2.2 Probability of precipitation intervals validation:

Eight PoP intervals have been validated. These intervals have been chosen in line with the colour scale delivered with the product:

- 0-5%: $0\% < \text{PoP} \leq 5\%$
- 5-15%: $5\% < \text{PoP} \leq 15\%$
- 15-25%: $15\% < \text{PoP} \leq 25\%$
- 25-35%: $25\% < \text{PoP} \leq 35\%$
- 35-45%: $35\% < \text{PoP} \leq 45\%$
- 45-55%: $45\% < \text{PoP} \leq 55\%$
- 55-65%: $55\% < \text{PoP} \leq 65\%$
- 65-100%: $65\% < \text{PoP} \leq 100\%$

For each probability interval only the rainy area with the selected probability has been taken into account. According to this, POD will always be 100%. Attention should be focused on FAR. A region with the probability of precipitation interval (A-B] should have $100\text{-B} \leq \text{FAR} < 100\text{-A}$. For a better understanding of this, see Figure 8.Imagine a precipitation probability pattern estimated like the one in the left part of the image. And imagine that the 25-35% probability interval is going to be validated. In this case only the green area in the central part of the image would be taken into account for validation, for both observation and estimation. In this case, the entire green area would be a rainy area according to the estimation, and so, a probability of detection of 100% would be assigned to this area. This assumption is represented at the right part of the image. To check whether this area has in effect a 25-35% precipitation probability, attention should be focused on false alarms. So, if the precipitation probability is 25-35%, then, false alarm ratio should be 65-75%.

Figure 8. Drawing example of probability of precipitation intervals validation

The categorical scores obtained are showed in Table 3.

Probability interval (%)	N (Day algorithm)	FAR (%) (Day algorithm)	N (Night algorithm)	FAR (%) (Night algorithm)
0-5	580028	87,28	487349	88,17
5-15	874949	79,97	1238899	85,49
15-25	573867	67,38	1286422	73,09
25-35	331008	54,53	1100344	60,86
35-45	327523	47,64	191587	50,72
45-55	281118	37,56	1719	41,42
55-65	114062	27,21	527	9,11
65-100	24139	19,50	91	5,49

Table 3. Categorical scores for PC algorithm probability of precipitation intervals

It can be observed that PC algorithm provides FAR scores lower than expected, most of all for the highest probability intervals. It should be noted that the highest probability intervals include lower number of cases, most of all in the case of the night-time algorithm that assigns PoP with lower confidences, which is in agreement with the results observed during the subjective validation. The FAR for PoPs higher than 50% are even lower with respect to the FARs from the PoPs lower than 50%.

It can be also observed that the higher quality of the day-time algorithm obtained due to the valuable information provided by the solar channels, leads into lower FAR values for each probability interval.

2.2.3 Probability of precipitation thresholds validation:

Seven probability of precipitation thresholds have been validated. These thresholds are: 5%, 15%, 25% , 35% , 45% , 55% and 65% probability of precipitation.

For this kind of validation, the whole validation area has been taken into account and only pixels with a probability of precipitation higher than the specified threshold have been taken as satellite rainy pixels, all the other pixels are taken as non-rainy.

Probability of precipitation threshold (%)	N	FAR (%)	POD (%)	CSI (%)	PC (%)
5	5254532	61,91	87,09	36,06	67,52
15	5254532	52,34	71,23	39,97	77,50
25	5254532	44,34	54,29	37,90	81,29
35	5254532	39,82	40,67	32,05	81,86
45	5254532	33,71	25,15	22,30	81,57
55	5254532	25,86	9,27	8,98	80,24
65	5254532	19,50	1,76	0,02	0,79

Table 4. Categorical scores for PC day-time algorithm taking as rainy pixels those with probability of precipitation higher than the threshold

Probability of precipitation threshold (%)	N	FAR (%)	POD (%)	CSI (%)	PC (%)
5	6179225	72,44	89,55	26,70	53,23
15	6179225	66,18	74,26	30,27	67,47
25	6179225	59,31	44,81	27,11	77,08
35	6179225	50,50	8,17	7,54	80,95
45	6179225	32,73	0,13	0,13	80,99
55	6179225	8,58	0,05	0,05	80,99
65	6179225	5,49	0,01	0,01	80,98

Table 5. Categorical scores for PC night-time algorithm taking as rainy pixels those with probability of precipitation higher than the threshold

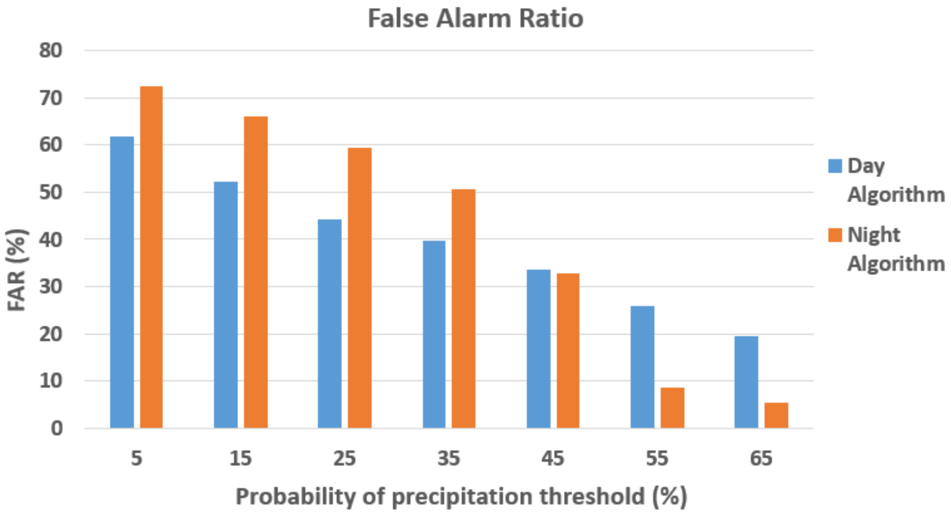

Figure 9. Comparison of day-time and night-time algorithms false alarm ratio

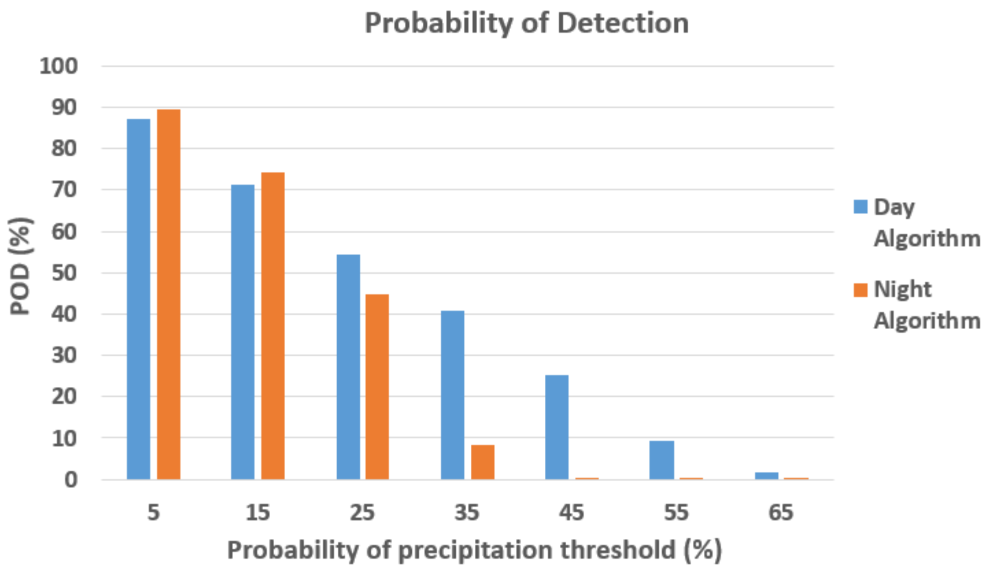

Figure 10. Comparison of day-time and night-time algorithms probability of detection

A clear better performance of the day-time algorithm over the night-time one can be observed in the graphs. Both lower FAR and higher POD have been obtained for the day-time algorithm for all the PoP thresholds. For 35% PoP and lower thresholds, POD is higher than FAR for the day-time algorithm. In the case of the night-time algorithm, this happens for 15% PoP threshold and the lower ones. For the higher PoP thresholds, scores get worse due to the low number of cases that reach these thresholds.

2.2.4 Conclusion

PC product catches most of the precipitation areas; however, probability of precipitation assigned, in a high number of cases, is underestimated. For this reason, although precipitation is detected, most of the time, is located in areas with PoPs lower than 55% for the day-time algorithm and lower than 45% in the case of the night-time one. PoPs higher than 65% are assigned few times in the case of the day-time algorithm and almost never in the case of the night-time one. So it is clear that the day-time algorithm provides better results than the night-time one due to the influence of the solar channels.

3. VALIDATION FOR CONVECTIVE RAINFALL RATE PRODUCT

This section contains the results obtained from the validation of the CRR product which is described in the "Algorithm Theoretical Basis Document for the Precipitation Product Processors of the NWC/GEO" *[RD 4]*.

3.1 SUBJECTIVE VALIDATION FOR CONVECTIVE RAINFALL RATE (CRR)

The monitoring of the precipitation pattern as well as its evolution is valuable information for the forecaster. In order to show the valuable information that CRR product can provide, a set of examples of CRR have been selected and compared to the radar estimations.

Next colour rain rate palate (mm/h) applies to figures 11-17 :

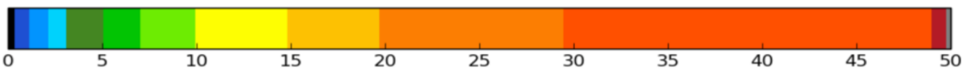

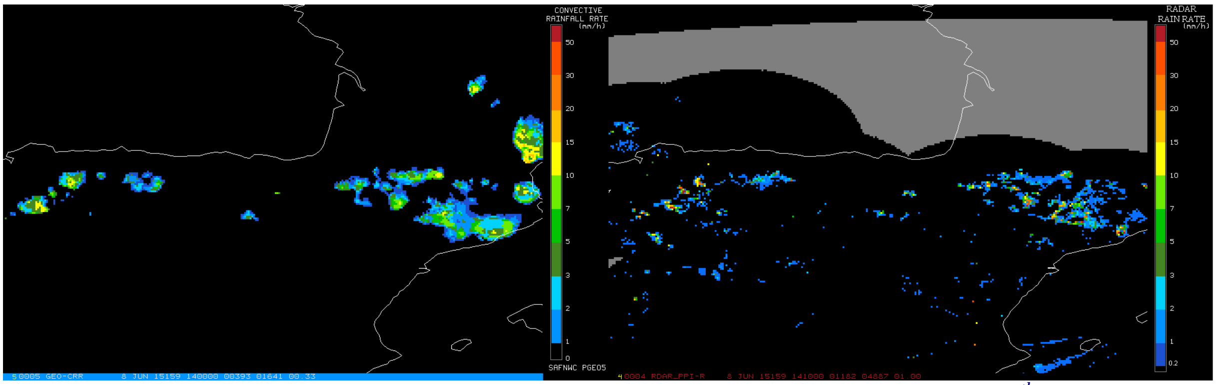

Figure 11. Comparison of CRR instantaneous rates product and radar (PPI) on 8th June 2015 at 10:00UTC

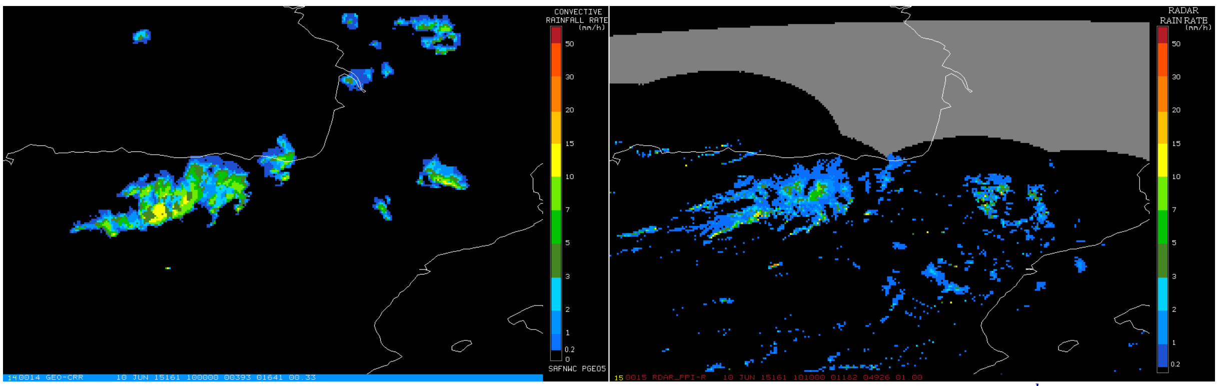

Figure 12. Comparison of CRR instantaneous rates product and radar (PPI) on 10th June 2015 at 10:00UTC

Figure 11 and Figure 12 show a couple of comparisons of CRR instantaneous rain rates with radar PPI product where most of the precipitation areas have been detected by CRR. Although the CRR precipitation pattern is quite similar to the radar one and the maxima of precipitation match well in location, maximum CRR rain rates are in general lower than the radar ones.

It is well known that for this kind of product directly based on cloud top radiances it is very difficult to detect the smallest precipitation nuclei. And it is also difficult to detect the lowest rain rates. It can be observed in the images that the rainy area is well depicted but sometimes is overestimated, being very similar to the cloud top structure. And it can also be observed a general underestimation of the highest rain rates.

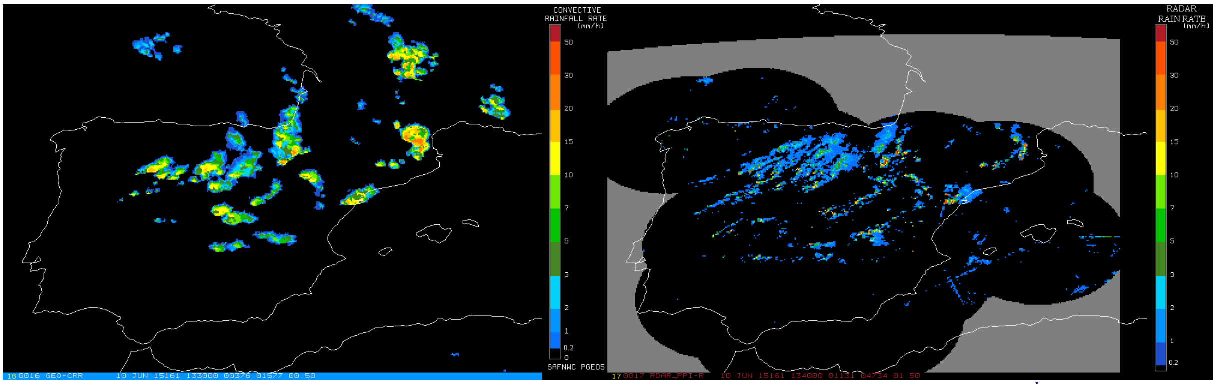

Figure 13. Comparison of CRR instantaneous rates product and radar (PPI) on 10th June 2015 at 13:30UTC

Figure 13 shows an example of a good performance of CRR product day-time algorithm. Although the smallest rain nuclei are missed by CRR, the precipitation pattern is very similar to the radar one and the maximum rain rates are also very similar.

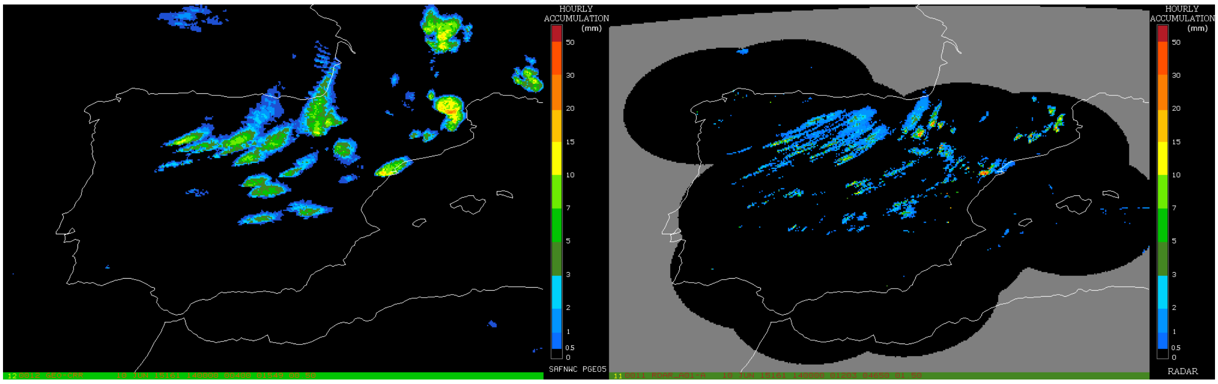

Figure 14. Comparison of CRR hourly accumulation product and radar hourly accumulation on 10th June 2015 at 14:00UTC

Figure 14 shows a comparison of hourly accumulation estimated by CRR and radar. Similar conclusions as in the case of instantaneous rain rates can be reached for hourly accumulations since hourly accumulations are obtained by using the instantaneous rain rates.

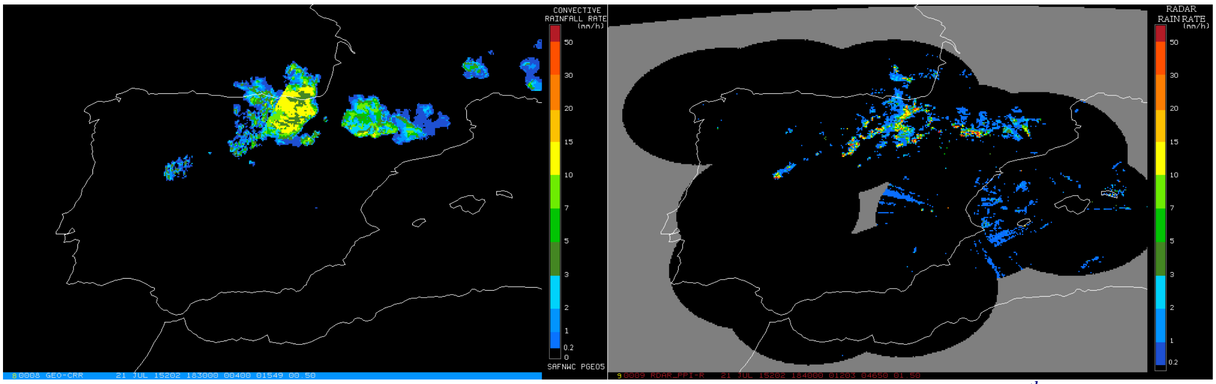

Figure 15. Comparison of CRR instantaneous rates product and radar (PPI) on 21th June 2015 at 18:30UTC

Figure 15 shows a CRR day-night algorithm transition. The day-time algorithm is displayed on the right side of the abrupt precipitation product transition. The night-time algorithm is displayed on the left side of this feature. It is quite clear through this example the main differences between both algorithms. Day-time algorithm provides a rain pattern more adjusted to the radar one while night-time one is more similar to the cloud top, overestimating rainy areas. Day-time algorithm provides better results due to the important information included in the visible channel related to the cloud optical thickness.

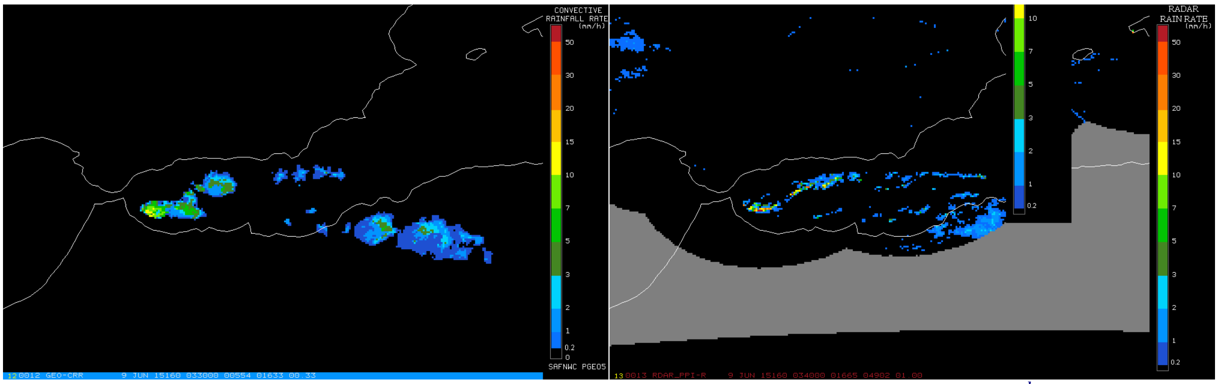

Figure 16. Comparison of CRR instantaneous rates product and radar (PPI) on 9th June 2015 at 03:30UTC

Figure 16 shows an example of the night-time algorithm. Although quality is not as good as in the case of the day-time one, precipitation areas are very similar to the radar one, and maximum rain rates are well located.

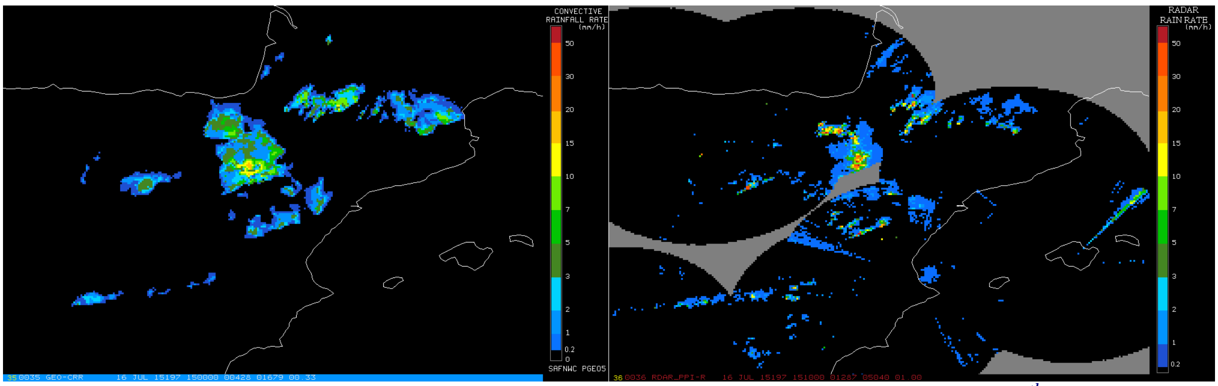

Figure 17. Comparison of CRR instantaneous rates product and radar (PPI) on 16th June 2015 at 15:00UTC

Figure 17 shows an example of the usefulness of CRR information when radar does not totally cover the studied area. Precipitation areas in those places covered by radar are similar and complementary information can be obtained through CRR out of those areas.

3.2 OBJECTIVE VALIDATION FOR CONVECTIVE RAINFALL RATE (CRR)

3.2.1 Validation Procedure

The objective instantaneous rain rates validation has been done against instantaneous rates taken from Spanish radar PPI data and the hourly accumulations have been done against radar hourly accumulations obtained from the 500m Pseudo-CAPPI. The original data in Lambert projection has been customary reprojected on the MSG projection using a bi-linear interpolation scheme.

Ground echoes in PPI scenes have been removed. To do that, a filter image, available as a radar product, has been used in order to remove ground echoes (windmills, …). For instantaneous products there exists the possibility to remove ground echoes, like anomalous propagation echoes, through the 10.8IR scene. A rain image has been obtained from the 10.8IR data using the basic AUTOESTIMATOR algorithm (Vicente et al., 1998). A pixel with significant radar echo is considered to be a ground echo and set to zero if no significant value is found in a 15x15 centred box in the AUTOESTIMATOR image.

Although satellite data have been used for decluttering the radar data, since this information has been used in a non-aggressive way, datasets are still independent enough for statistical comparison.

In the instantaneous cases, since CRR product addresses convective situations, only images with convective echoes should be validated. In order to select those images, when in the ECHOTOP image the ratio between the number of pixels with ECHOTOP higher than 6 Km and the number of pixels with ECHOTOP higher than 0 Km is lower than 15%, the radar images have been rejected. This procedure tends to discard non-convective precipitation.

Images with convective situations can also include non-convective echoes. In order to validate only the convective ones, a validation area has been selected taking into account the convective area that has been calculated in each image. To do that, PPI and ECHOTOP images have been used. The convective area in the instantaneous images has been made up of 15x15 pixels boxes centred on pixels that reach a top of 6 km and a rainfall rate of 3 mm/h simultaneously. In the hourly accumulations, the validation area has been chosen adding the validation areas in the corresponding instantaneous images. As some CRR rainy pixels can appear out of the convective area, these pixels have been added to the validation area in order to include all the possible false alarms.

The perfect matching between images will never be reached so a smoothing process in a 3x3 pixels base has been done. The horizontal resolution of the pixels are 3kms at satellite point. Then a pixel by pixel (every three pixels) comparison has been carried out. The definition of the statistics computed can be checked at ANNEX 1: .

The CRR values have been obtained applying all the corrections with the default values *[RD 4]*. The fields for the moisture, parallax and orographic corrections have been extracted from ECMWF at 0.5 x 0.5 degree spatial resolution, every 3h.

The dataset used for the validation of both algorithms contains 78 days with convective events along 2008. Accuracy and categorical statistics described in ANNEX 1: have been computed for instantaneous rain rates and for hourly accumulations.

3.2.2 Instantaneous Rain Rates

According to the procedure described above, the statistical accuracy measurements are shown in the following table:

Algorithm	N	Mean (mm/h)	ME (mm/h)	MAE (mm/h)	RMSE (mm/h)
3 - Variables	832614	0,58	0,54	1,19	2,97
2 - Variables	877299	0,62	0,82	1,55	3,18

Table 6. Accuracy measurements for instantaneous rates

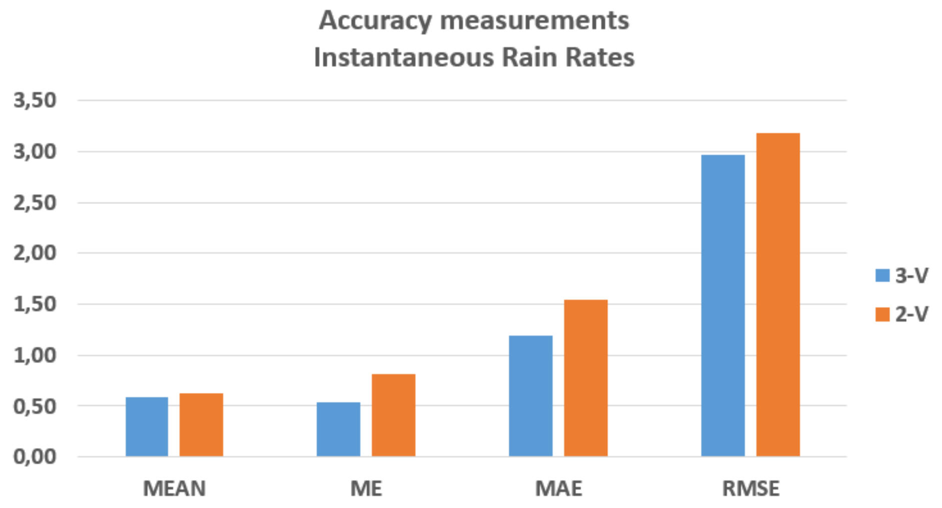

Figure 18. Accuracy measurements for CRR instantaneous rates

Although both day-time and night-time algorithms provide similar results, it can be observed a slight better performance in the day-time algorithm according to the results showed in Figure 18. This can be explained, as seen during the subjective validation, because day-time algorithm adjust better precipitation areas reducing error with respect to the night-time ones.

Categorical scores for CRR can be obtained assuming that values higher than or equal to 0.2 mm/h for instantaneous rates are considered rainy. Results are shown in Table 7.

Algorithm	FAR (%)	POD (%)	CSI (%)	PC (%)
3 - Variables	34,13	63,26	47,64	64,55
2 - Variables	45,53	53,74	37,08	54,57

Table 7. Categorical scores for CRR instantaneous rates

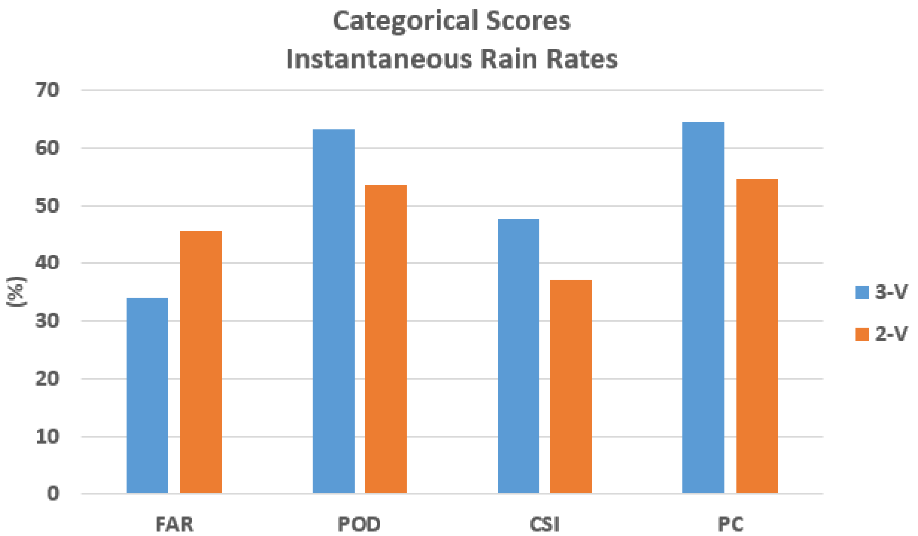

Figure 19. Categorical scores for CRR instantaneous rates

Figure 19 also brings to light the better estimations of the day-time algorithm that provides lower FAR and higher POD than the night-time one. These results, showed also in Table 7, fulfil the FAR and POD target values defined in the "NWCSAF Product Requirements document "*[AD. 4]*.

3.2.3 Hourly accumulations

Accuracy measurements, obtained statistically as explained above, for hourly precipitation accumulations are shown in Table 8.

Algorithm	N	Mean (mm/h)	ME (mm/h)	MAE (mm/h)	RMSE (mm/h)
3 - Variables	465555	0,37	0,43	0,80	1,96
2 - Variables	598562	0,40	0,57	0,99	2,19

Table 8. Accuracy measurements for CRR hourly accumulations

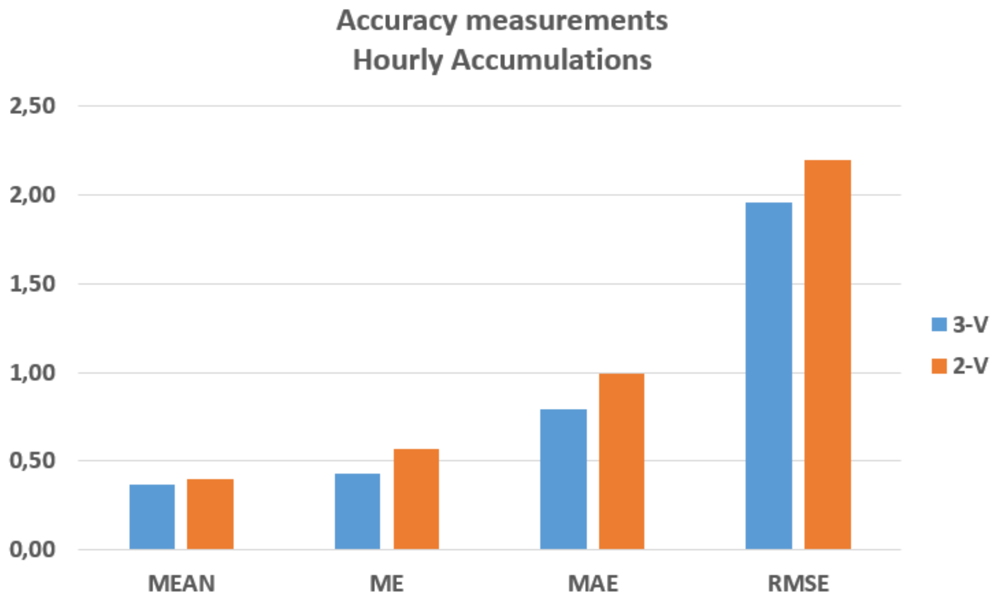

Figure 20. Accuracy measurements for CRR hourly accumulations

Since hourly accumulations have as a base the instantaneous rain rates, similar results are expected. Figure 20 show that accuracy measurements take lower values for hourly accumulations than for instantaneous rain rates. This happens because hourly accumulations fields are smoother than instantaneous rain rates ones. Better performance of the day-time algorithm with respect to the night-time one can be seen.

Categorical scores can be obtained assuming that values higher than or equal to 0.2 mm/h for hourly precipitation accumulations are considered rainy. Results are shown in Table 9.

Algorithm	FAR (%)	POD (%)	CSI (%)	PC (%)
3 - Variables	51,07	65,33	38,84	63,17
2 - Variables	58,19	56,43	31,61	56,29

Table 9. Categorical scores for CRR hourly accumulations

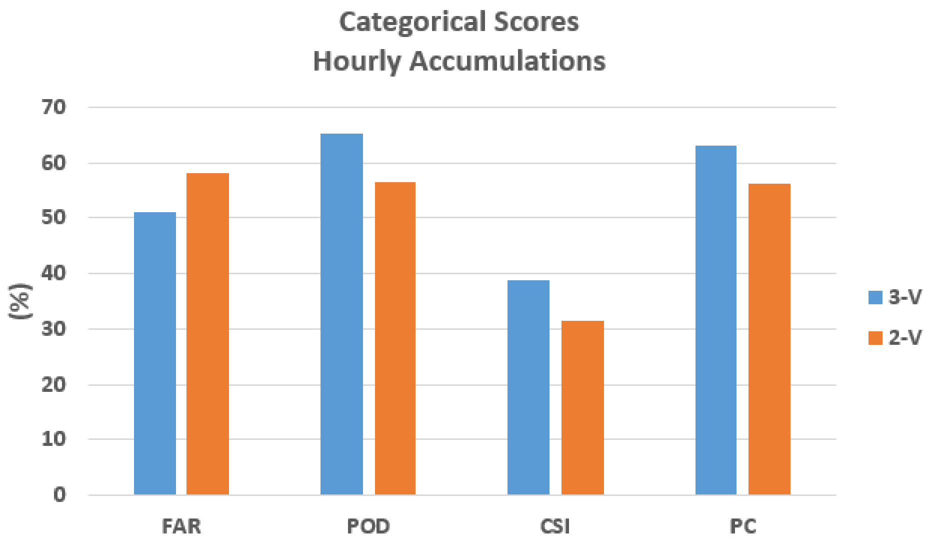

Figure 21. Categorical scores for CRR hourly accumulations

As for categorical scores, Figure 21 shows also the better estimations provided by the day-time algorithm and results from Table 9 fulfil the FAR and POD target values defined in the "NWCSAF Product Requirements document "*[AD. 4]*.

3.2.4 Conclusion

Algorithm	Threshold Accuracy FAR (%)	Target Accuracy FAR (%)	Optimal Accuracy FAR (%)	FAR (%)
3 - Variables	<60	<40	<38	34.13
2 - Variables	<65	<50	<44	45.53

Table 10. Comparison of CRR instantaneous rates FAR scores and FAR accuracy values defined in the NWCSAF Product Requirement table

Algorithm	Threshold Accuracy POD (%)	Target Accuracy POD (%)	Optimal Accuracy POD (%)	POD (%)
3 - Variables	>40	>53	>87	63.26
2 - Variables	>35	>47	>85	53.74

Table 11. Comparison of CRR instantaneous rates POD scores and POD accuracy values defined in the NWCSAF Product Requirement table

Algorithm	Threshold Accuracy FAR (%)	Target Accuracy FAR (%)	Optimal Accuracy FAR (%)	FAR (%)
3 - Variables	<65	<55	<45	51.07
2 - Variables	<70	<60	<50	58.19

Table 12. Comparison of CRR hourly accumulations FAR scores and FAR accuracy values defined in the NWCSAF Product Requirement table

Algorithm	Threshold Accuracy POD (%)	Target Accuracy POD (%)	Optimal Accuracy POD (%)	POD (%)
3 - Variables	>45	>58	>95	65.33
2 - Variables	>37	>50	>90	56.43

Table 13. Comparison of CRR hourly accumulations POD scores and POD accuracy values defined in the NWCSAF Product Requirement table

4. VALIDATION FOR PRECIPITATING CLOUDS FROM CLOUD PHYSICAL PROPERTIES PRODUCT

This section contains the results obtained from the validation of the PC-Ph product which is described in the "Algorithm Theoretical Basis Document for the Precipitation Product Processors of the NWC/GEO "*[RD 4]*.

The validation procedure consists of two parts:

- ✓ Subjective validation
- ✓ Objective validation

The subjective validation compares 2 images: The Spanish composite radar with the PC-Ph product.
The objective validation is based in a pixel-pixel comparison between the radar data and the PC-Ph product.

Within the objective validation two different methods have been applied:

- ➢ Categorical validation
- ➢ Intervals validation

The first one is the traditional categorical way of computing the POD and FAR scores. The second method is a validation that divides the PC-Ph in intervals. Then, for each interval the number of rainy pixels is calculated.

4.1 SUBJECTIVE VALIDATION FOR PRECIPITATING CLOUDS FROM CLOUD PHYSICAL PROPERTIES (PC-PH)

In this section a visual check is possible by comparing the probability of precipitation (PoP) obtained from the PC-Ph algorithm against the radar data.

This subjective study has focused on convective episodes throughout 2016. Different day and night slots have been chosen to depict the PC-Ph general behaviour.

A pair of images are shown to subjectively validate the PC-Ph product: Rainy pixels extracted from the Spanish radar reflectivity composition and the probability of precipitation product.

The image on the left side correspond with the reflectivity of the radar (PPI image) and the image on the right side correspond with the PC-Ph output (see Figures 22-27 and Figures 30-32).

On the right side of the image of figures 28 and 29 (day algorithm), pixels where the probability of precipitation is equal or higher to 20% are painted in red colour. On the right side of the image of figures 33 and 34 (night algorithm) pixels with probability of precipitation equal or higher to 40% are also painted in red.

4.1.1 DAY

For an easier visualization, PC-Ph day output pixels with NO DATA have been plotted in black, due to an undefined phase or No data or corrupted data input.

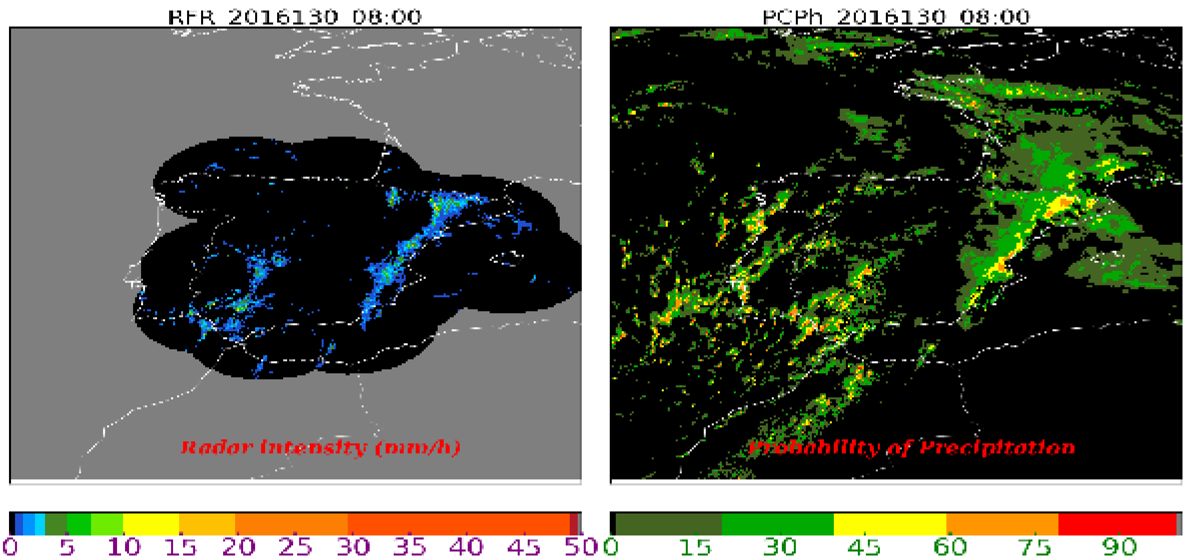

Figure 22. Comparison of radar (PPI) and PC-Ph day product on 9th May 2016 at 08:00UTC

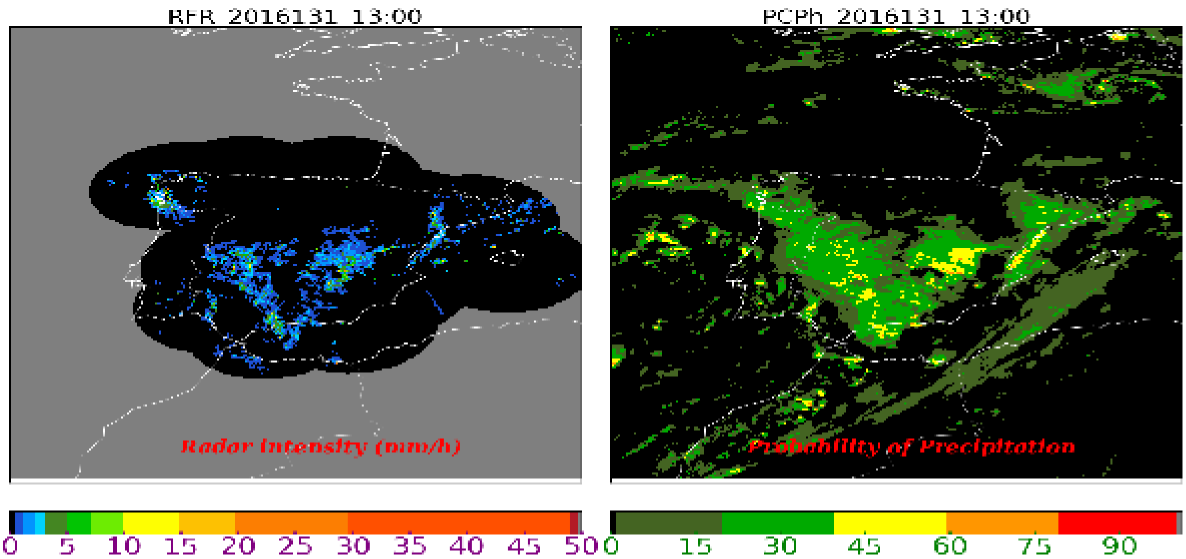

Figure 23. Comparison of radar (PPI) and PC-Ph day product on 10th May 2016 at 13:00UTC

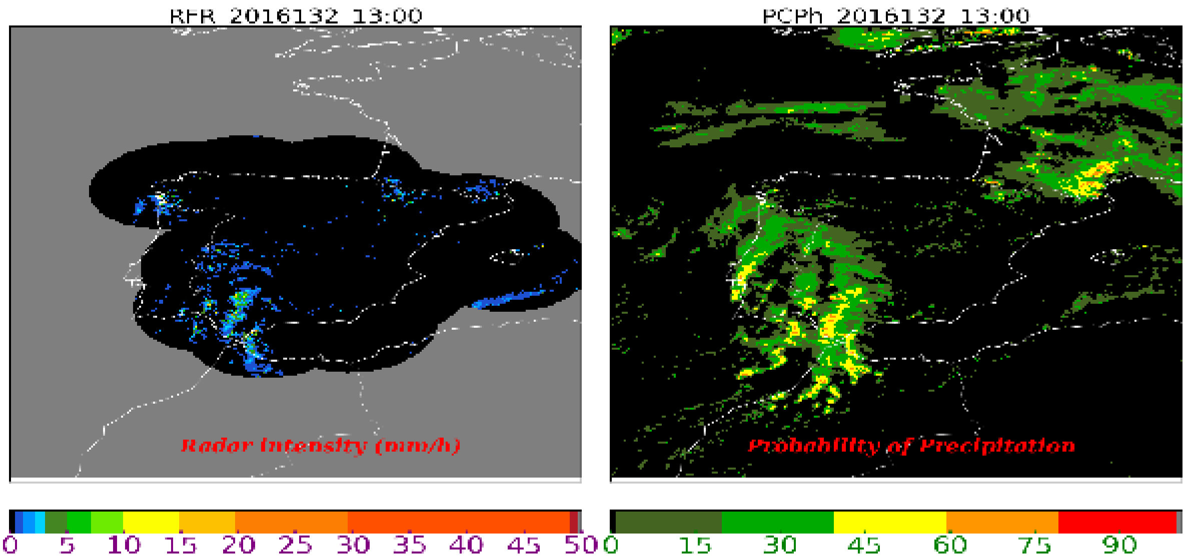

Figure 24. Comparison of radar (PPI) and PC-Ph day product on 11th May 2016 at 13:00UTC

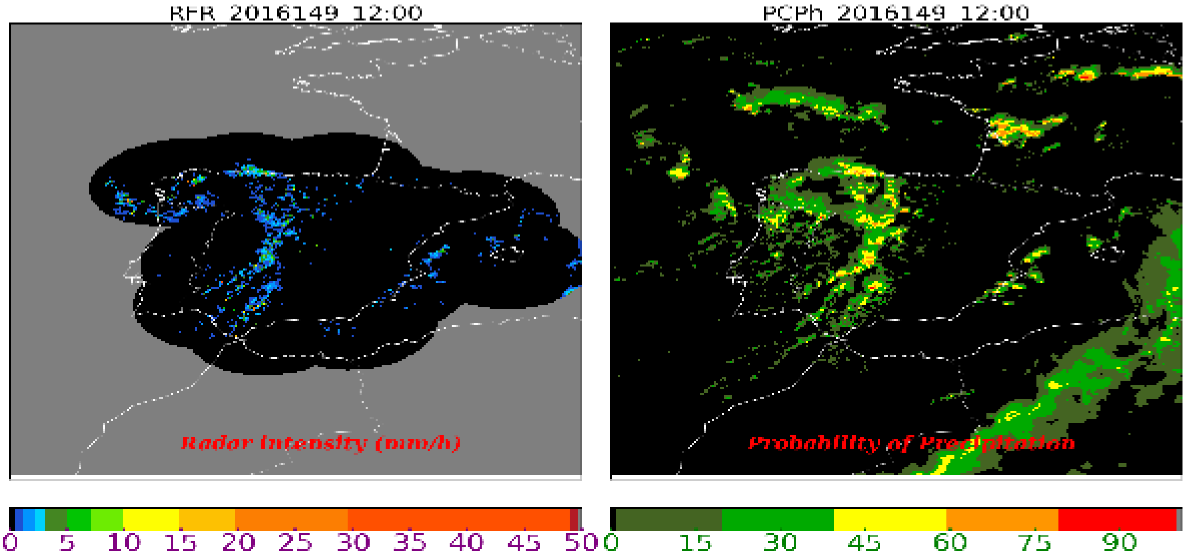

Figure 25. Comparison of radar (PPI) and PC-Ph day product on 28th May 2016 at 12:00UTC

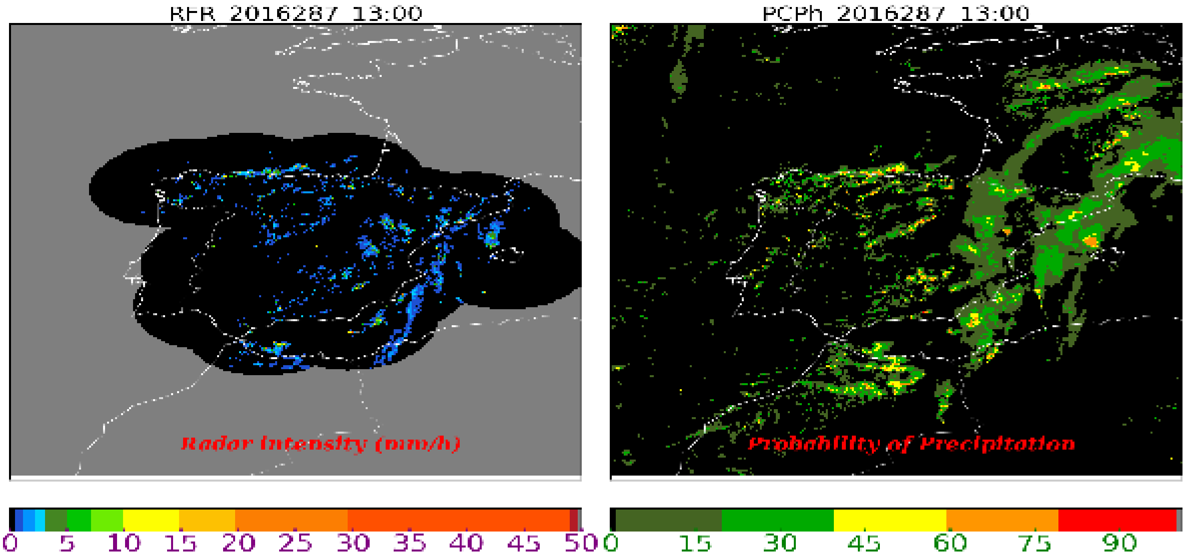

Figure 26. Comparison of radar (PPI) and PC-Ph day product on 13th October 2016 at 13:00UTC

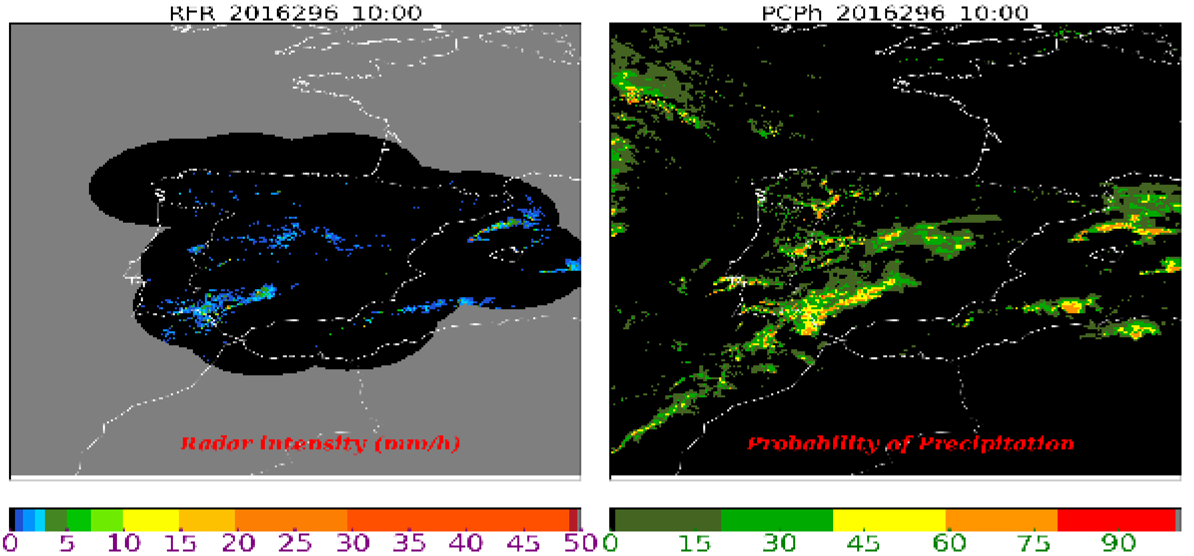

Figure 27. Comparison of radar (PPI) and PC-Ph day product on 22th October 2016 at 10:00UTC

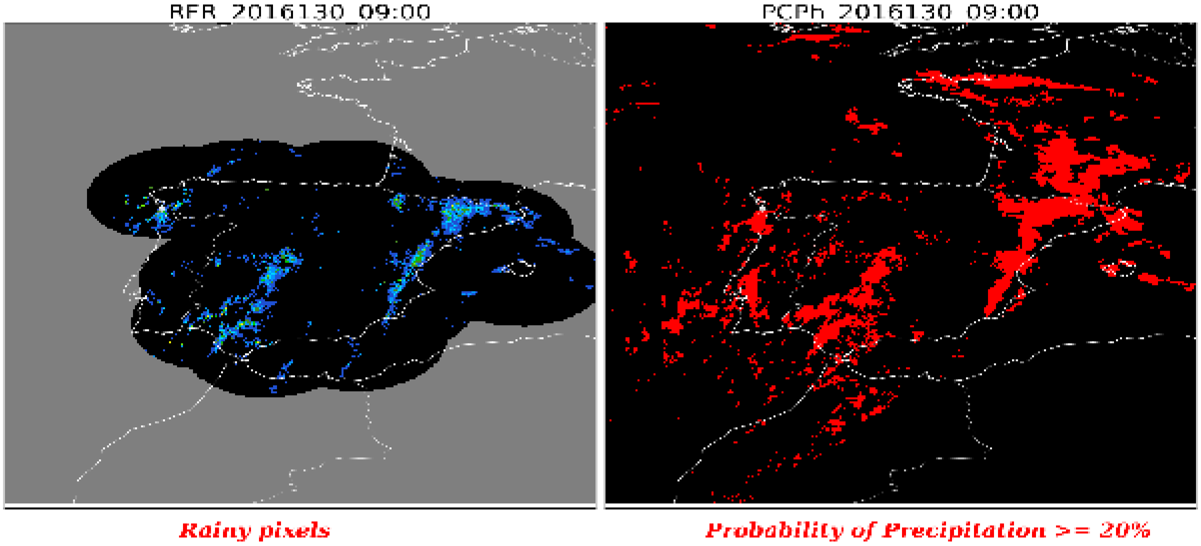

Figure 28. Comparison of radar (PPI) and probability of precipitation equal or higher to 20% extracted from PC-Ph product on 9th Mayo 2016 at 09:00UTC

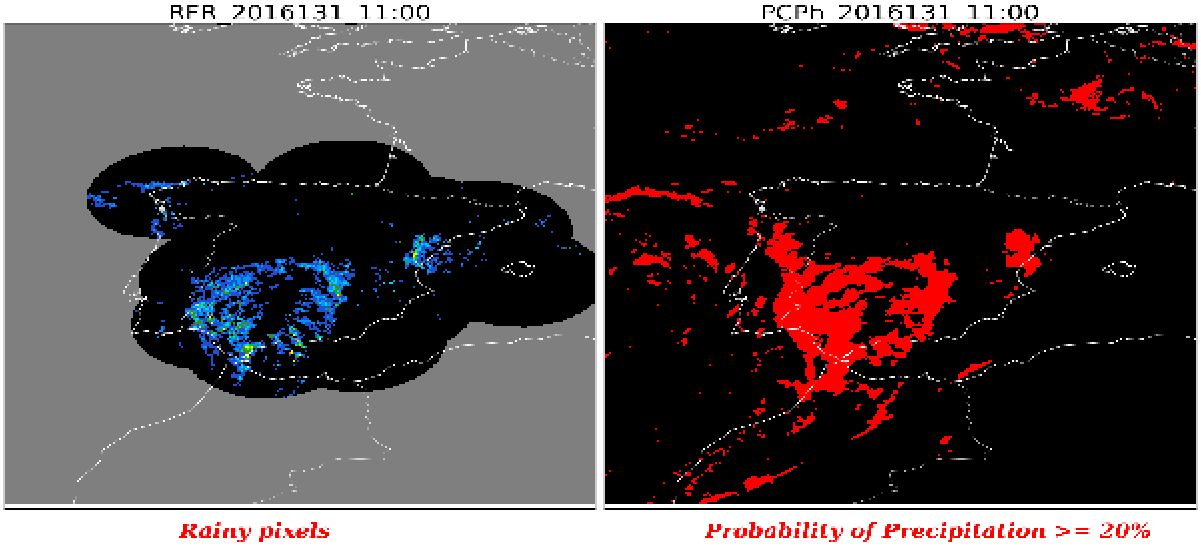

Figure 29. Comparison of radar (PPI) and probability of precipitation equal or higher to 20% extracted from PC-Ph product on 10th May 2016 at 11:00UTC

As it can be noticed there is a really good visual matching between those areas where the PPI radar assigns rain rates equal or higher to 0.2 mm/h and those areas where the PC-Ph product estimate probability of precipitation equal or higher to 20 %.

4.1.2 NIGHT

For an easier visualization, PC-Ph night output pixels with NO DATA have been plotted in black, due to an undefined phase or No data or corrupted data input.

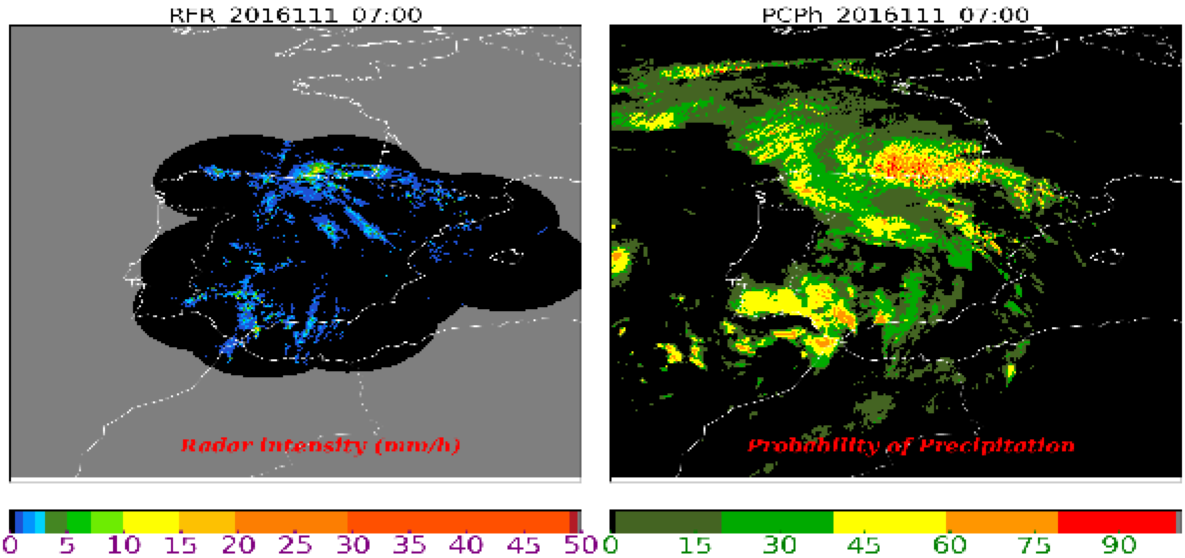

Figure 30. Comparison of radar (PPI) and PC-Ph day product on 20th April 2016 at 07:00UTC

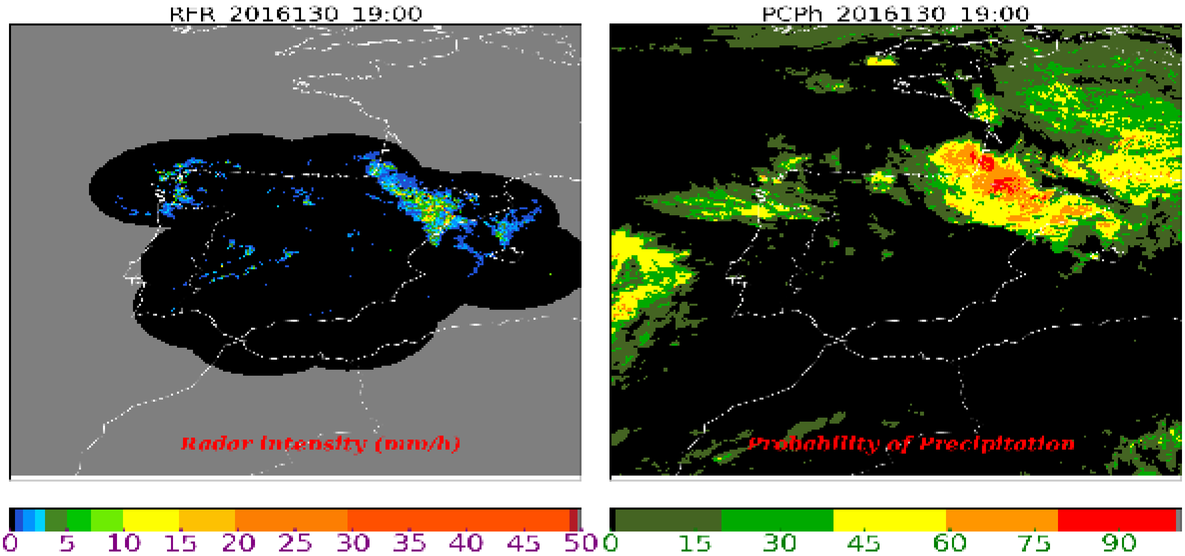

Figure 31. Comparison of radar (PPI) and PC-Ph day product on 9th May 2016 at 19:00UTC

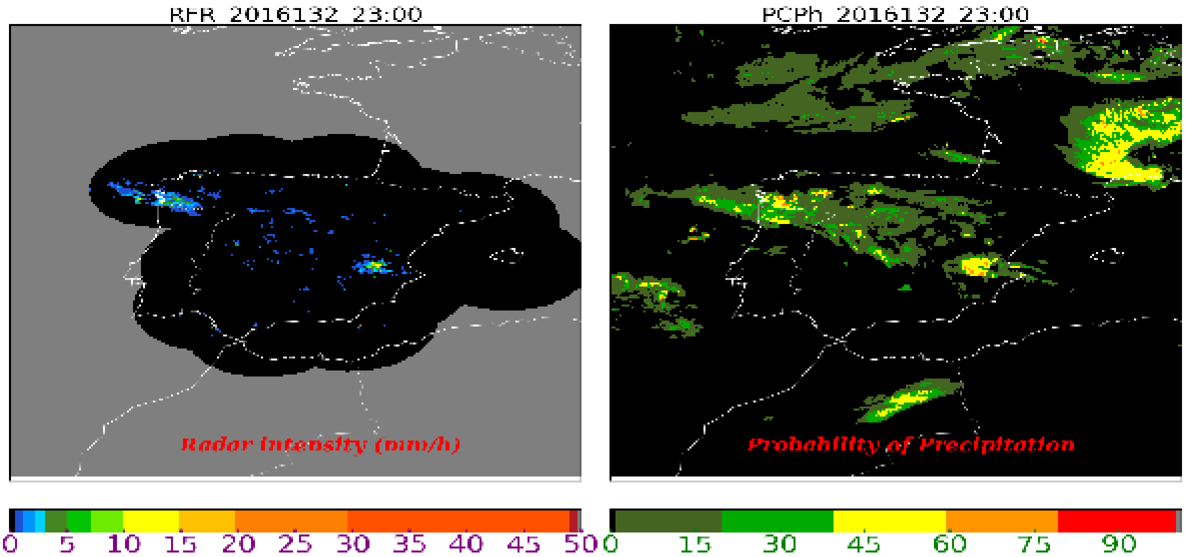

Figure 32. *Comparison of radar (PPI) and PC-Ph day product on 11th May 2016 at 23:00UT*

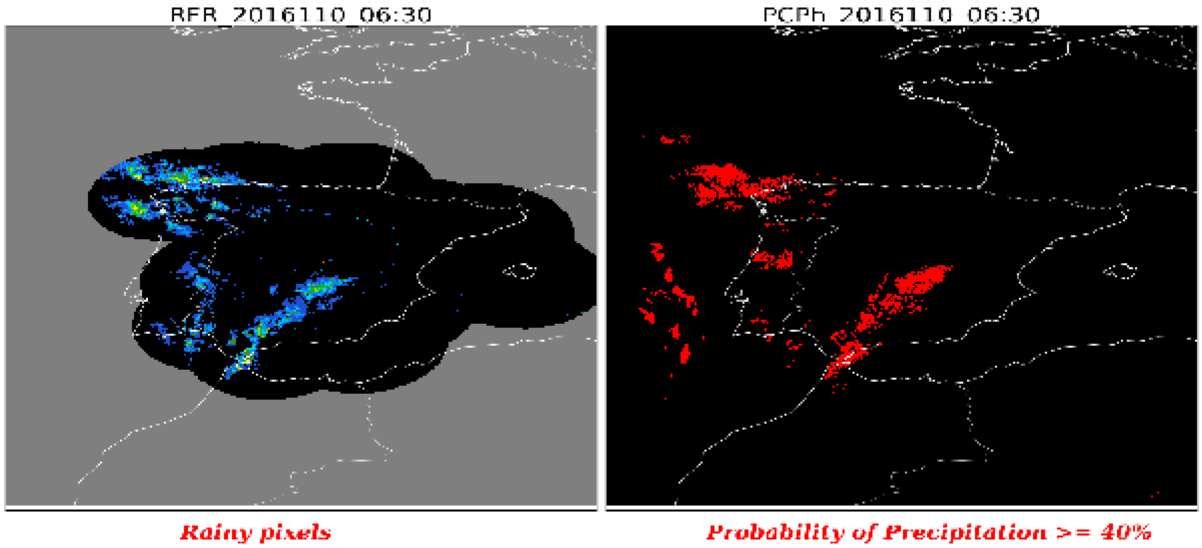

Figure 33. Comparison of radar (PPI) and probability of precipitation equal or higher to 40% extracted from PC-Ph product on 19th April 2016 at 6:30UTC

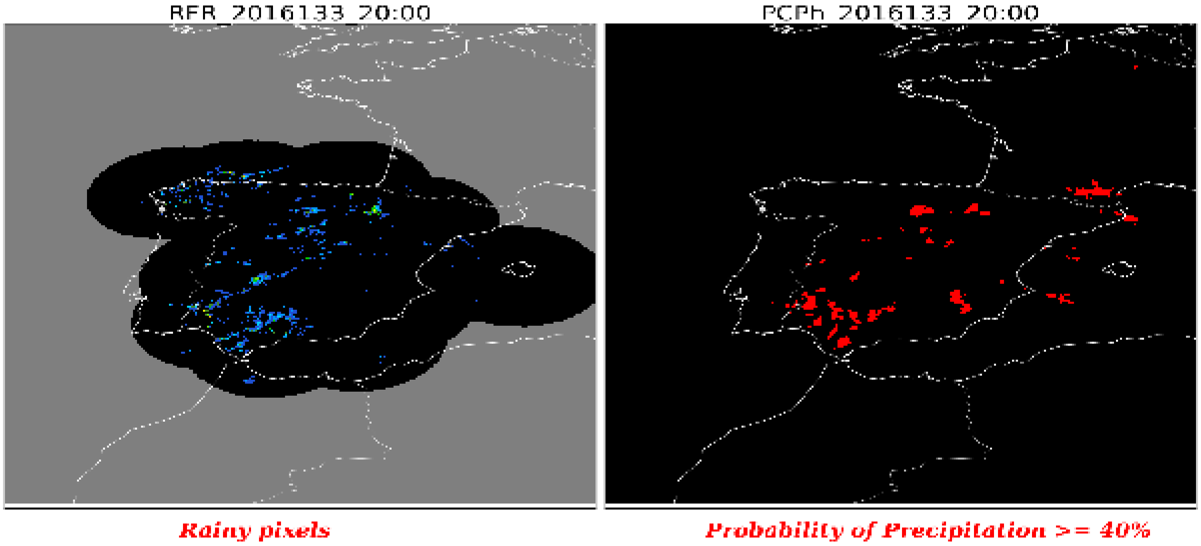

Figure 34. Comparison of radar (PPI) and probability of precipitation equal or higher to 40% extracted from PC-Ph product on 12th May 2016 at 20:00UTC

While the visual matching between the radar and the probability of precipitation at day happens when the probability of precipitation is equal or higher to 20%, at night the visual matching happens with probabilities equal or higher to 40%.

4.2 Objective validation for Precipitating Clouds from Cloud Physical Properties (PC-Ph)

4.2.1 Validation Procedure

Two objective validations have been made comparing the PC-Ph algorithm against the Spanish composite radar. The first one is the traditional way of obtaining the POD and FAR indicators included in the “NWCSAF Product Requirements Document” [AD 4]. The second one is an alternative way and it has been previously explained in a document named after “Adaptation of GEO-PC-Ph product for MTG” [RD 6]. In both cases a day night distinction have been included.
Every slot has been classified as day slot, night slot or mixed, depending on the number of day or night pixels of each image. In order to evaluate the day algorithm separately from the night algorithm, mixed slots have been discarded. This way a day or night slot only contains pixels of the same category.

The PC-Ph product has been calibrated with a list of days throughout 2015 that accomplished at least one of two criteria. They are based on echotop (ET) and rainfall rate (RFR). Another list of days has been created throughout 2016, with the same criteria as 2015, to validate the product.

RFR in mm/h is obtained from the lowest Plan Position Indicator (PPI) of the radar using the Marshal-Palmer relation, $Z=200R^{1.6}$, where Z ($mm^6\,mm^{-3}$) is the reflectivity factor and R($mm\,h^{-1}$) is the rainfall rate. Echotop values in km. correspond with the maximum height that echoes bigger than 12dBz are able to reach.

First criterion: A particular day is included in the calibration and validation list if the percentage of pixels with ET>6km. with respects to pixels with ET>0 km exceeds the threshold of 65% at least for one slot of this day.

Second criterion: It is calculated the proportion of radar pixels with RFR>=0.2mm/h with respect to the whole image. Whenever at least one slot of a day reaches the percentage limit of 8% the day was also included in the calibration and validation list.

Since Microphysical Cloud Top parameters used by the PC-Ph algorithm have been computed only for sun zenith angles lower than 70º, this validation has been undertaken under the same condition.

The PC-Ph product assigns NO DATA value to those pixels with undefined phase according to the phase output of the CMIC product, which means that no information on whether the cloud consists of water or ice is available. Those pixels have been excluded in the algorithm validation.

Radar data, which are in Lambert Projection with a 1km*1km pixel resolution, have been converted into the MSG projection, using a bi-linear interpolation. The horizontal resolution of the MSG pixels are 3kms at satellite point. Parallax correction has been applied to the PC-Ph product. As a perfect matching between Radar and MSG images is not possible, a smoothing process in 3x3 boxes pixels has been done. The threshold to consider a pixel to rainy has been fixed at 0.2 mm/h because detection of very light rain rates using GEO satellite data is not possible.

A radar quality image has been used as a filter image to get rid of spurious echoes, such as windmill echoes. Anomalous propagation echoes have been removed through the 10.8IR scene. A rain image has been obtained from the 10.8IR data using the basic AUTOESTIMATOR algorithm (Vicente et al., 1998). A pixel with significant radar echo is considered to be a ground echo and set to zero if no significant value is found in a 15x15 box centred in the AUTOESTIMATOR image.

Before calculating the POD and FAR scores, correct negatives (see Table 29 in ANNEX 1: VERIFICATION METRIC section) have been filtered because they represent a large number of the data population, reduce speed computing and they are not involved in the categorical scores formula.

Due to the temporal resolution of the SEVIRI data in the normal mode, there are four PC-Ph outputs available every hour. The Spanish radar network generates a set of instantaneous products every 10 minutes. The MSG scanning over Spain is done over 10 minutes after the slot hour. The only way to temporally match PC-Ph product with radar images is choosing 0 and 30 minutes PC-Ph images corresponding to 10 and 40 minutes radar images respectively. This way 15 and 45 minutes PC-Ph images, which do not temporally match with the radar images, have not been used in the validation process.

Both categorical and accuracy statistic have been used to validate de product. They are explained in ANNEX 1: VERIFICATION METRIC.

4.2.2 Probability of precipitation categorical thresholds validation

Three different probability of precipitation thresholds have been stablished to check the dependence of the categorical validation process with those thresholds. The three chosen thresholds are: 20%, 30% and 40% probability of precipitation for the PC-Ph product.
Within all of the following PC-Ph categorical thresholds validation, rainy pixels from the radar are fixed to at least 0.2 mm/h in every of them.

It can be noticed that reducing the threshold from 30% to 20% of probability of precipitation, the target object, fixed in the "NWCSAF Product Requirements document"[AD4], is achieved for both day and night algorithm.

DAY:

- 20 % probability of precipitation threshold:

N	POD (%)	FAR (%)	CSI (%)	PC (%)
1658229	**73.91**	**30.2**	56.0	70.59

Table 14. Categorical scores in convective episodes for PC-Ph day algorithm taking as rainy pixels those with probability of precipitation higher than 20%.

- 30% probability of precipitation threshold:

N	POD (%)	FAR (%)	CSI (%)	PC (%)
1658229	50.71	**22.86**	44.08	67.42

Table 15. Categorical scores in convective episodes for PC-Ph day algorithm taking as rainy pixels those with probability of precipitation higher than 30%.

- 40% probability of precipitation threshold:

N	POD (%)	FAR (%)	CSI (%)	PC (%)
1658229	26.43	**18.95**	24.9	56.61

Table 16. Categorical scores in convective episodes for PC-Ph day algorithm taking as rainy pixels those with probability of precipitation higher than 40%.

NIGHT:

- 20 % probability of precipitation threshold:

N	POD (%)	FAR (%)	CSI (%)	PC (%)
5070332	**59.12**	**36.13**	44.3	59.39

Table 17. Categorical scores in convective episodes for PC-Ph night algorithm taking as rainy pixels those with probability of precipitation higher than 20%.

- 30% probability of precipitation threshold:

N	POD (%)	FAR (%)	CSI (%)	PC (%)
5070332	44.49	**33.50**	36.34	57.43

Table 18. Categorical scores in convective episodes for PC-Ph night algorithm taking as rainy pixels those with probability of precipitation higher than 30%.

- 40% probability of precipitation threshold:

N	POD (%)	FAR (%)	CSI (%)	PC (%)

5070332	32.06	**30.97**	28.03	55.02

Table 19. Categorical scores in convective episodes for PC-Ph night algorithm taking as rainy pixels those with probability of precipitation higher than 40%.

4.2.3 Probability of precipitation intervals validation

While categorical scores have been evaluated in convective areas in the past, new interval validation scores have been calculated in all areas, convective and non-convective. These scores have been described in the document [RD6] "Adaptation of PC-Ph product for MTG".

One weak point of using categorical scores (POD, FAR…), it is that they are not only influenced by the quality of the product, but also they have a strong dependence with the data distribution.
A new validation method is applied to consider comparing the frequency distributions of PC-Ph and radar rain rate to mitigate the strong dependency on data distribution.

The way of calculating this new validation method consists of the following:
There are two long arrays of data, one with the rainfall rates (from the radar) and the other one with the PC-Ph product. First of all, the PC-Ph database is divided in fixed intervals and then we compare the frequency of radar data higher to 0.2mm/h in each category or interval with the expected frequency (men value of each interval: 5%, 15%, 25%,...)

Results using these new scores are shown in the next tables.

PC-Ph range (%)	Cases	Cases with rain (%)	Error (%)
0-10	4375163	10.62	5.62
10-20	2453384	20.42	5.42
20-30	1810501	40.44	15.44
30-40	898837	59.68	24.68
40-50	319895	69.07	24.07
50-60	136032	74.30	19.30
60-70	54799	78.28	13.29
70-80	7747	82.91	7.91
80-90	21	Not enough cases	
90-100	0	Not enough cases	

Table 20. Accuracy scores for PC-Ph day algorithm in all areas

PC-Ph range (%)	Cases	Cases with rain (%)	Error (%)
0-10	22383800	14.43	9.43
10-20	11196176	19.07	4.08
20-30	5769660	23.51	-1.48
30-40	3715795	27.42	-7.58
40-50	2661781	32.96	-12.04
50-60	1801827	41.59	-13.41
60-70	364811	53.52	-11.48
70-80	59062	67.50	-7.50
80-90	6954	82.56	-2.44

90-100	362	93.65	-1.35

Table 21. Accuracy scores for PC-Ph night algorithm in all areas

As we can see the database has been divided in different PC-Ph intervals. For each interval, the number of rainy pixels is calculated and then the error is evaluated by subtracting the mean value of the interval from the previous value. PC-Ph product is considered perfect when, among all the pixels in each interval of probability of precipitation (by the product PC-Ph), 0-10%,10-20%,…,90-100%, the percentage of then that are really rainy (by radar) is exactly the mean value of the interval, 5%,15%,…,95%.

For example, in the first interval (0-10) %, PC-Ph day product is considered to be perfect if 5% of all the pixels were rainy. In this case there are 46464 rainy pixels over 4375163, that means the 10.62 percentage of the pixels are rainy pixels (0.2mm/h or higher). Then the error equals to 10.62-5=5.62. The more probability of precipitation, estimated by the PC-Ph product, the more rainy pixels are found in each interval.

4.2.4 Conclusions

PC-Ph product provide us with a general good depiction of the precipitation areas. According to the categorical validation FAR score is within the limits for both day and night, but POP score is only achieved if the threshold is reduced to 20%. (Green bold colour is chosen when stablished limits are fulfilled).
With respect to the new accuracy validation, on the one hand, we observe that the day algorithm tends to slightly underestimate the probability of precipitation and it doesn´t cover the whole probability intervals range. On the other hand, night algorithm covers all the probability PC-Ph intervals with a slightly overestimation when the probability of precipitation goes from 40 % to 70%.
With respect to the visual matching, at day, there is a good visual accordance between the radar the PC-Ph product when the probability of precipitation is equal or higher to 20% and at night, the visual matching happens with probabilities equal or higher to 40%

5. VALIDATION FOR CONVECTIVE RAINFALL RATE FROM CLOUD PHYSICAL PROPERTIES PRODUCT

This section contains the results obtained from the validation of the CRR-Ph product which is described in the “Algorithm Theoretical Basis Document for the Precipitation Product Processors of the NWC/GEO” *[RD 4]*.

The validation procedure consists of two parts:

- ✓ Subjective validation
- ✓ Objective validation

The subjective validation compares 2 images: The Spanish composite radar with the CRR-Ph product.

The objective validation is based in a pixel-pixel comparison between the radar data and the CRR-Ph product. As far as the objective validation is concerned, different categorical scores have been calculated (see annex I at the end)

5.1 SUBJECTIVE VALIDATION FOR CONVECTIVE RAINFALL RATE FROM CLOUD PHYSICAL PROPERTIES (CRR-PH)

The monitoring of the precipitation pattern as well as its evolution is a valuable information for the forecaster. In order to check this information, visual comparisons between CRR-Ph and radar images have been done. A summary of these comparisons containing different study cases that represent the general behaviour of these algorithms have been selected for this purpose.

5.1.1 DAY

A pair of images are shown to subjectively validate the CRR-Ph day product: The image on the left side corresponds with the reflectivity of the radar (PPI image) and the image on the right side corresponds with the rain rates of the CRR-Ph product (see Figures 35-48).

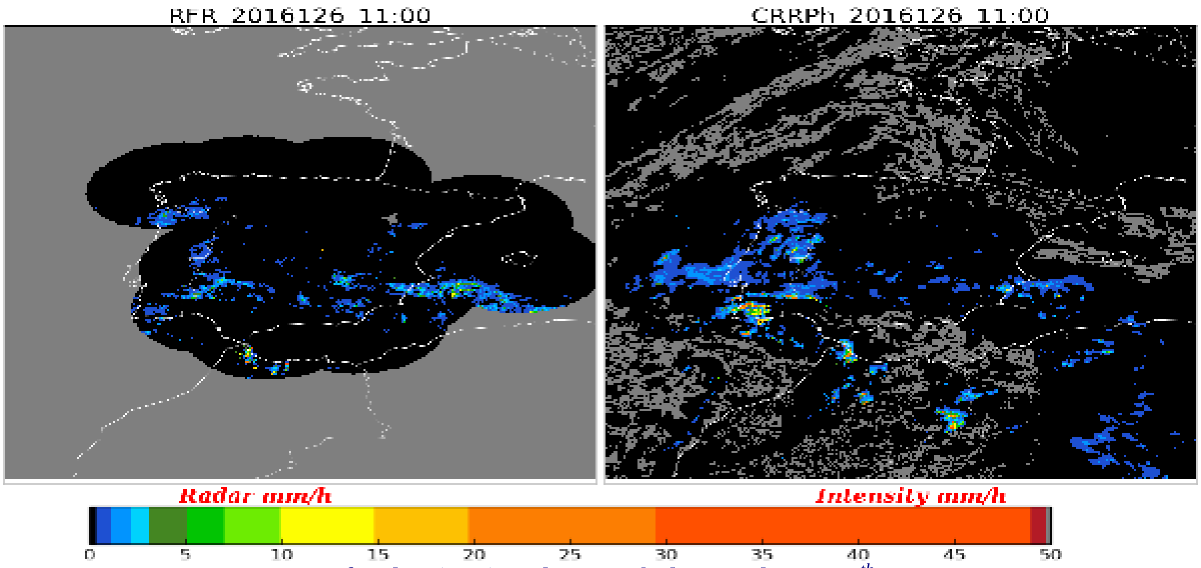

Figure 35. Comparison of radar (PPI) and CRR-Ph day product on 5th May 2016 at 11:00UTC

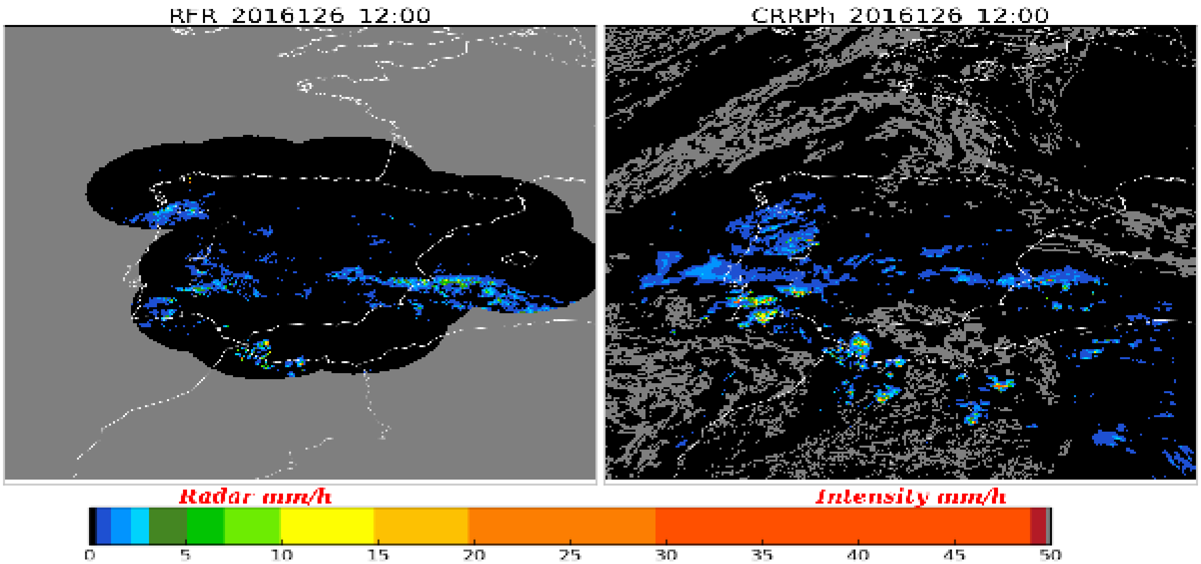

Figure 36. Comparison of radar (PPI) and CRR-Ph day product on 5th May 2016 at 12:00UTC

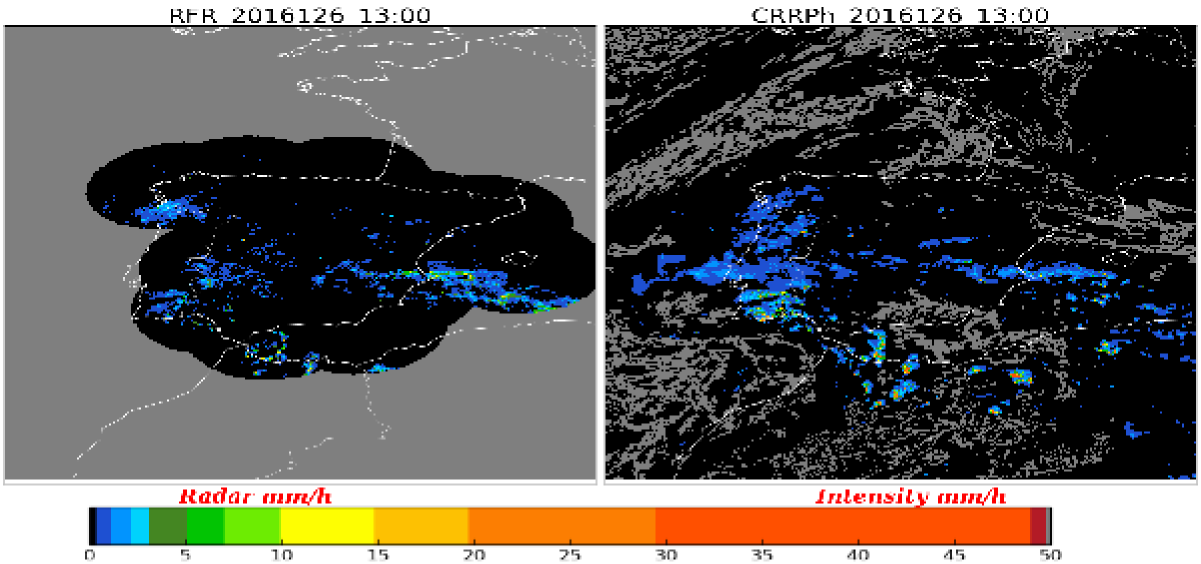

Figure 37. Comparison of radar (PPI) and CRR-Ph day product on 5th May 2016 at 13:00UTC

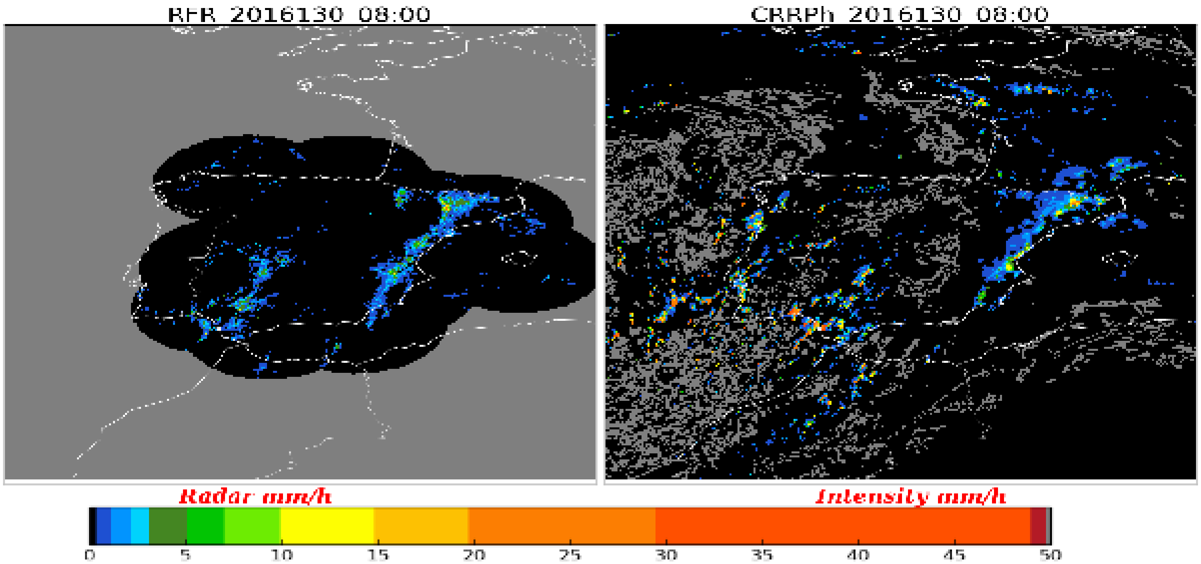

Figure 38. Comparison of radar (PPI) and CRR-Ph day product on 9th May 2016 at 08:00UTC

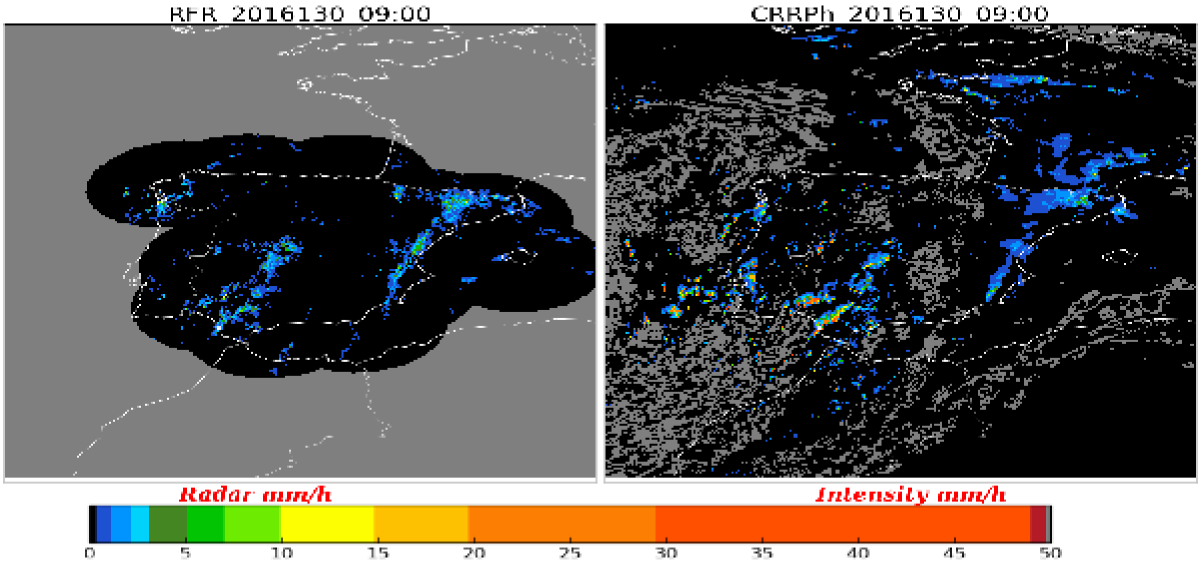

Figure 39. Comparison of radar (PPI) and CRR-Ph day product on 9th May 2016 at 09:00UTC

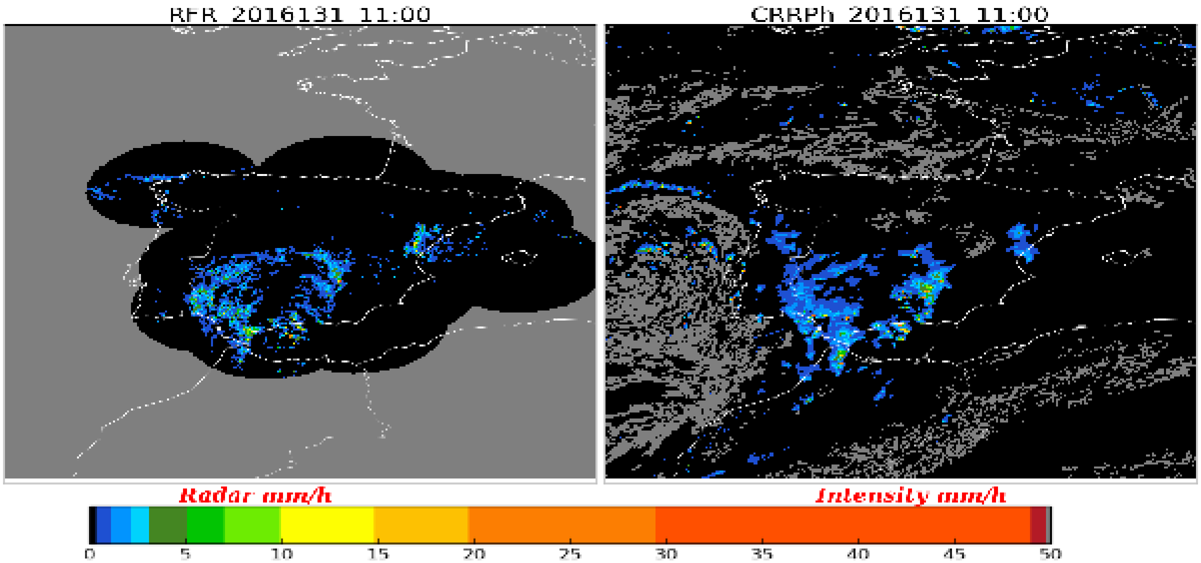

Figure 40. Comparison of radar (PPI) and CRR-Ph day product on 10th May 2016 at 11:00UTC

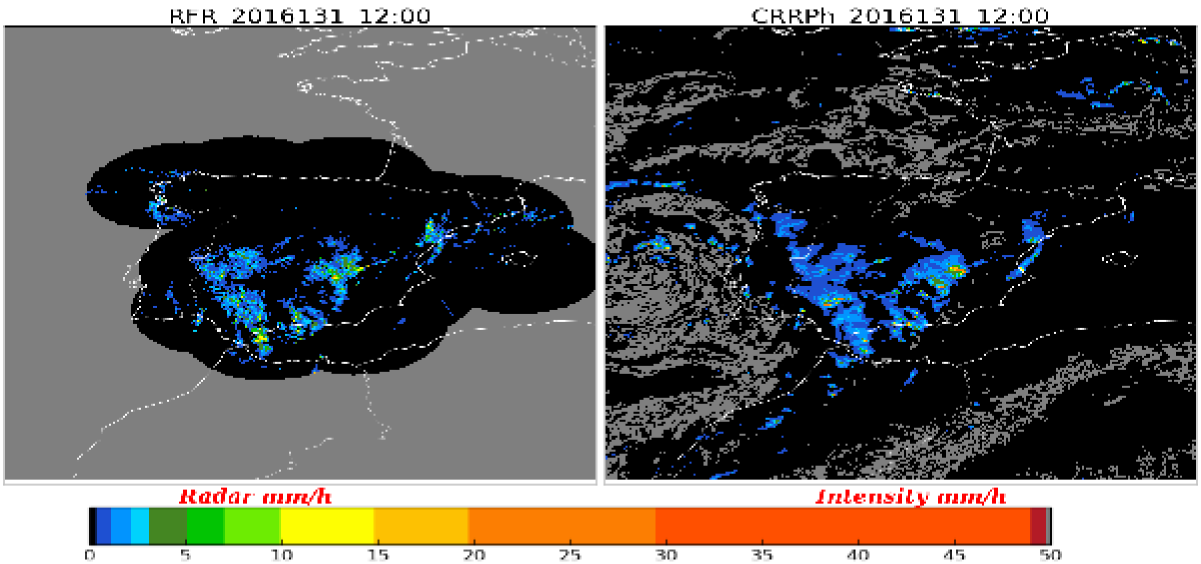

Figure 41. Comparison of radar (PPI) and CRR-Ph day product on 10th May 2016 at 12:00UTC

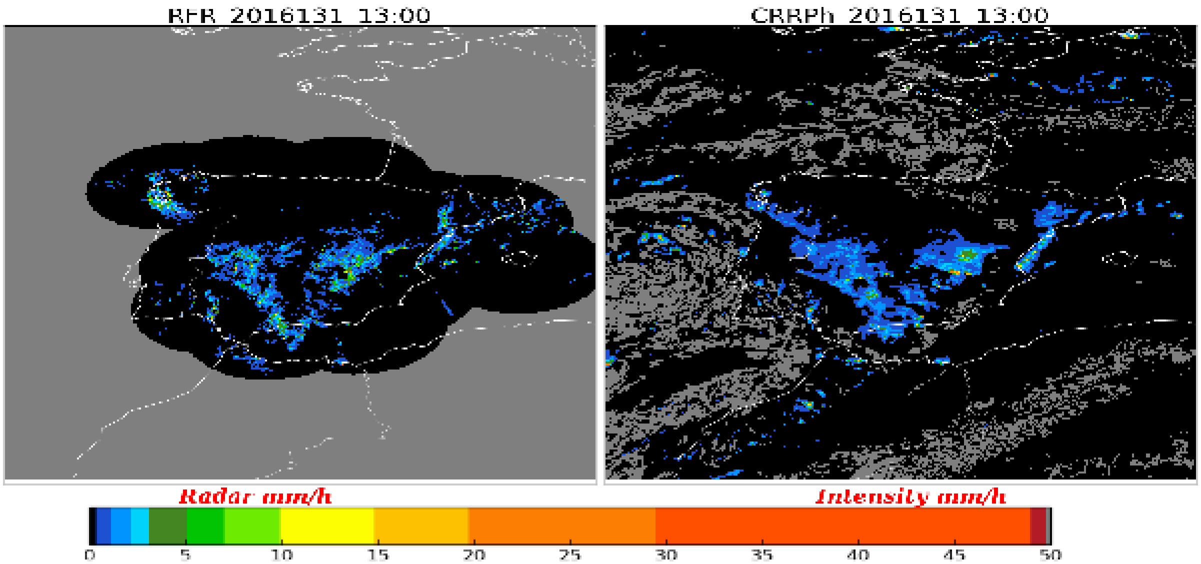

Figure 42. Comparison of radar (PPI) and CRR-Ph day product on 10th May 2016 at 13:00UTC

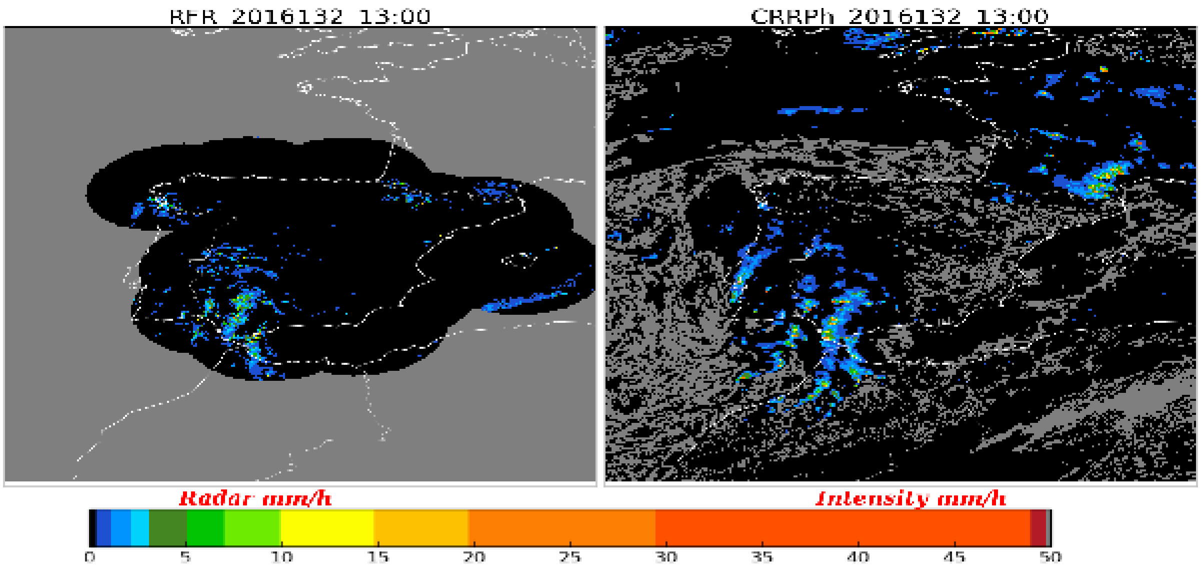

Figure 43. Comparison of radar (PPI) and CRR-Ph day product on 11th May 2016 at 13:00UTC

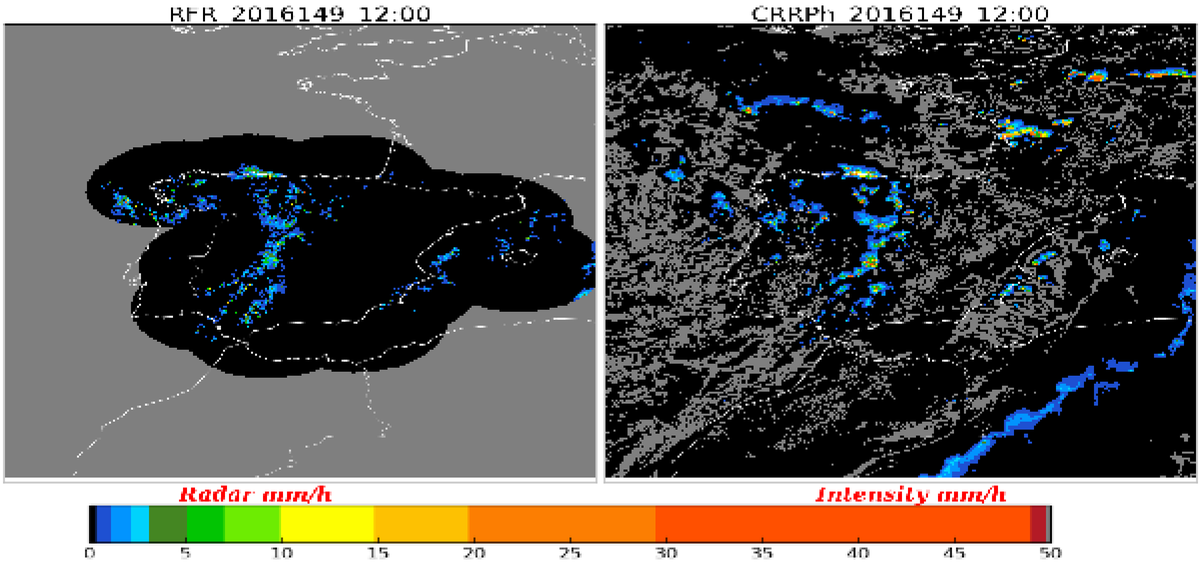

Figure 44. Comparison of radar (PPI) and CRR-Ph day product on 28th May 2016 at 12:00UTC

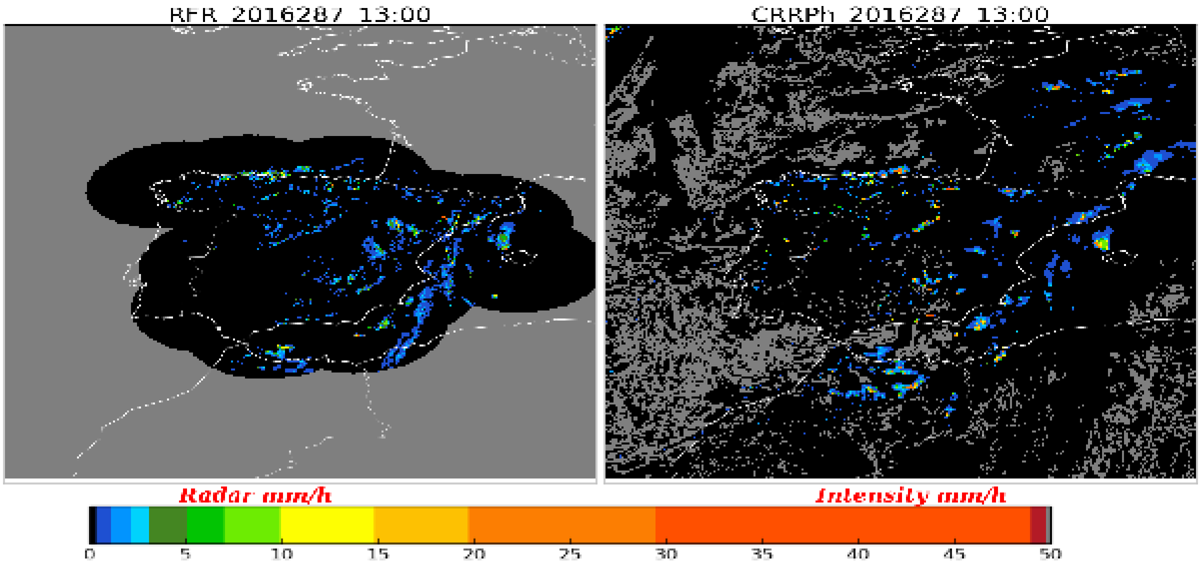

Figure 45. Comparison of radar (PPI) and CRR-Ph day product on 13th October 2016 at 13:00UTC

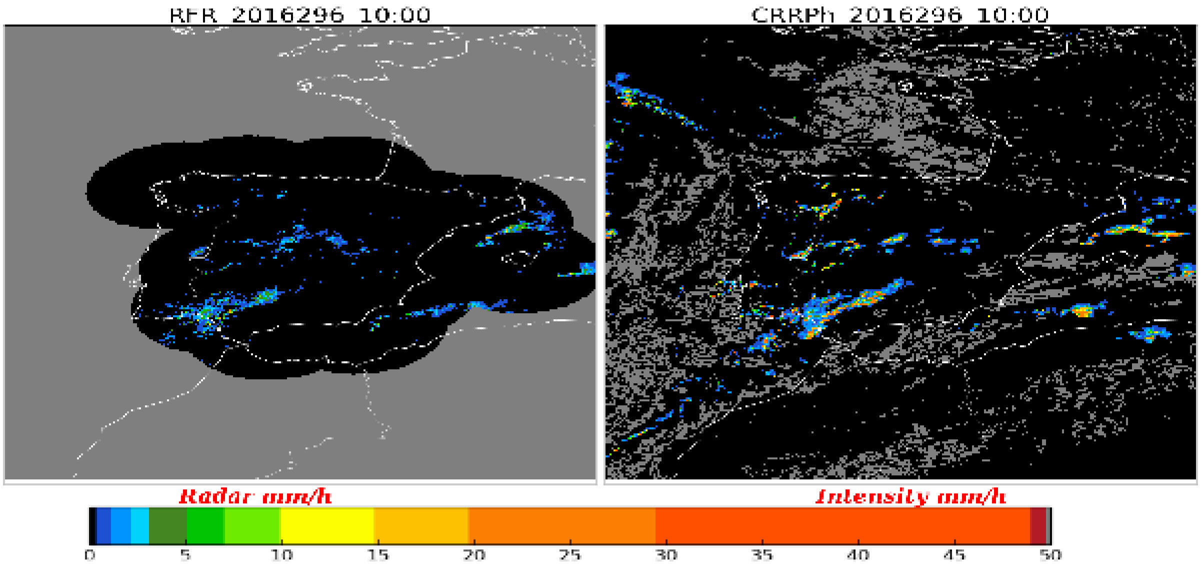

Figure 46. Comparison of radar (PPI) and CRR-Ph day product on 22th October2016 at 10:00UTC

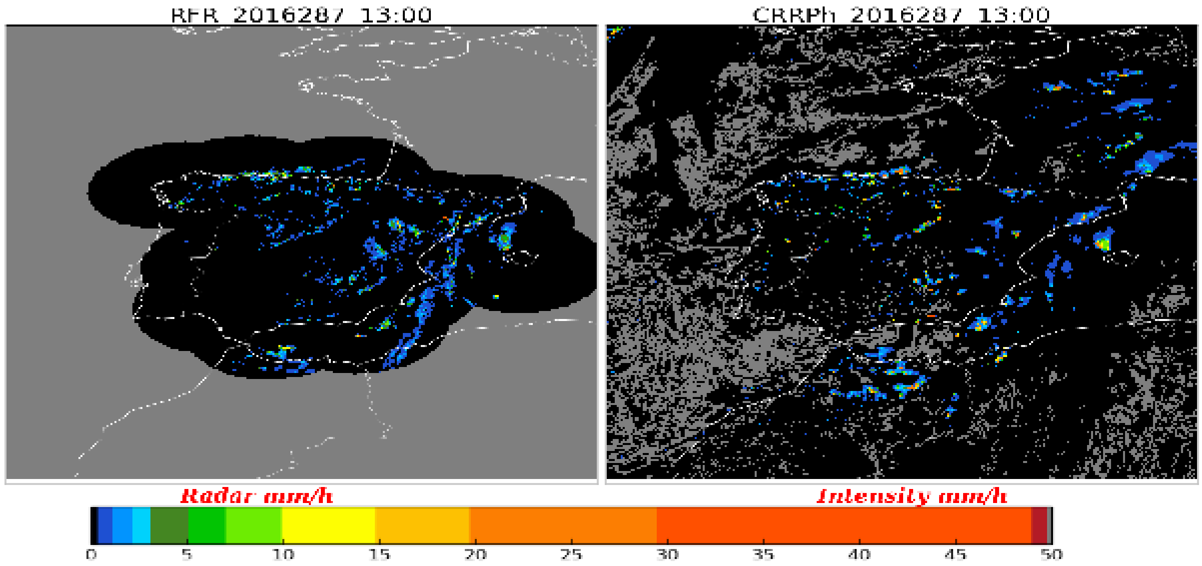

Figure 47. Comparison of radar (PPI) and CRR-Ph day product on 13th October 2016 at 13:00UTC

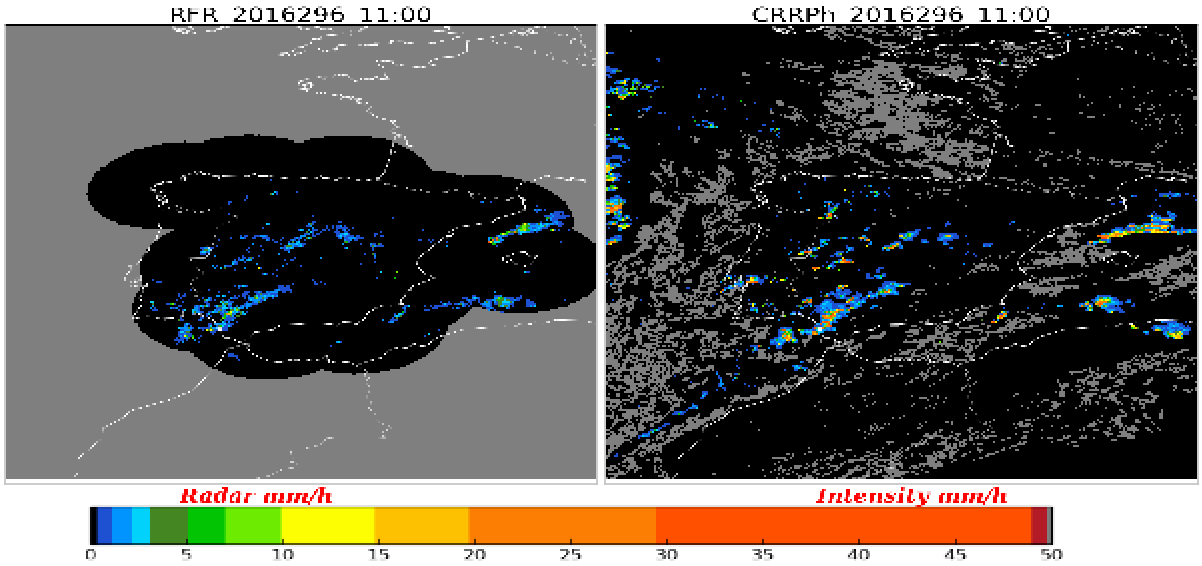

Figure 48. Comparison of radar (PPI) and CRR-Ph day product on 22th October 2016 at 11:00UTC

As it can be noticed , there is a general good visual matching between the radar and the CRR-Ph day algorithm.

5.1.2 NIGHT

With the aim of visually validate the CRR-Ph night product to images are plotted. The one on the left side corresponds with the reflectivity of the radar (PPI image) and the image on the right side corresponds with the rain rates of the CRR-Ph product.

For an easier visualization, it have been plotted in black those pixels with NO DATA output corresponding with an undefined phase or No data or corrupted data input.

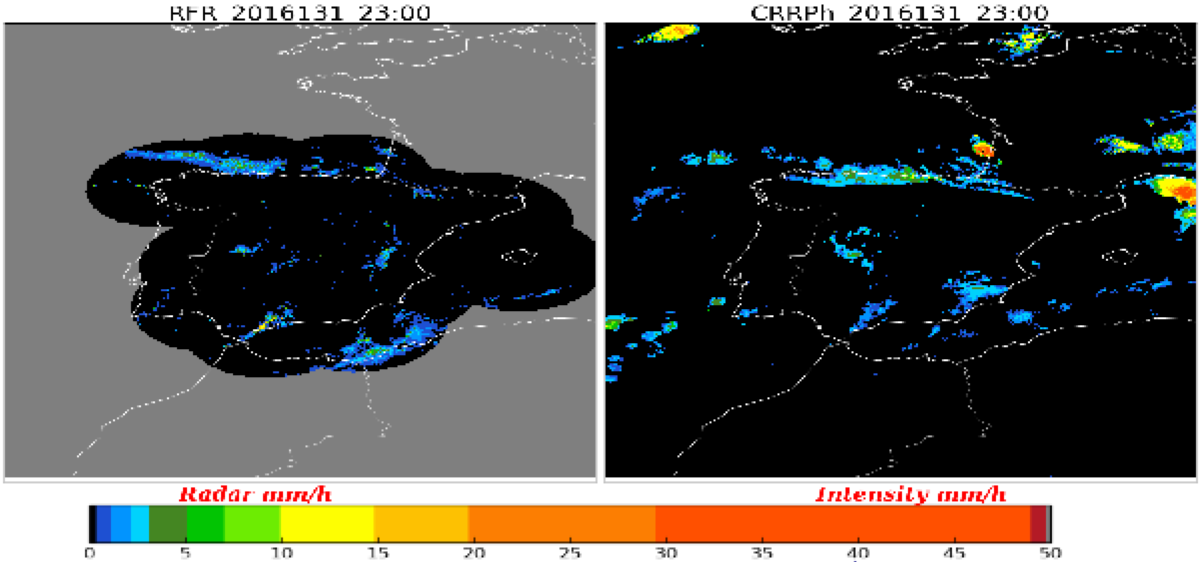

Figure 49. Comparison of radar (PPI) and CRR-Ph night product on 10th May 2016 at 23:00UTC

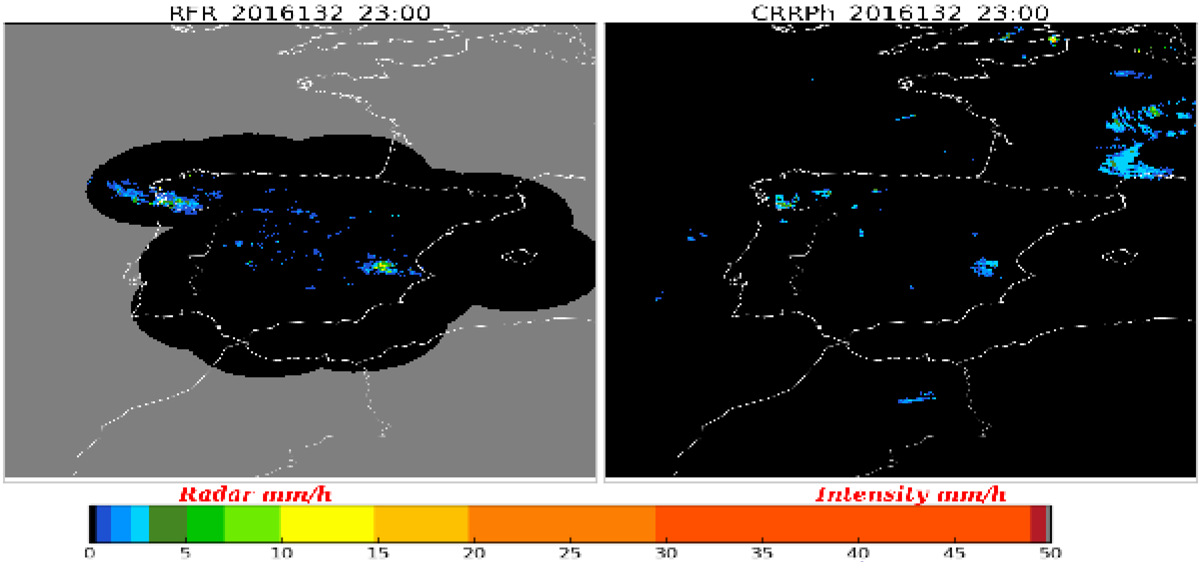

Figure 50. Comparison of radar (PPI) and CRR-Ph night product on 11th May 2016 at 23:00UTC

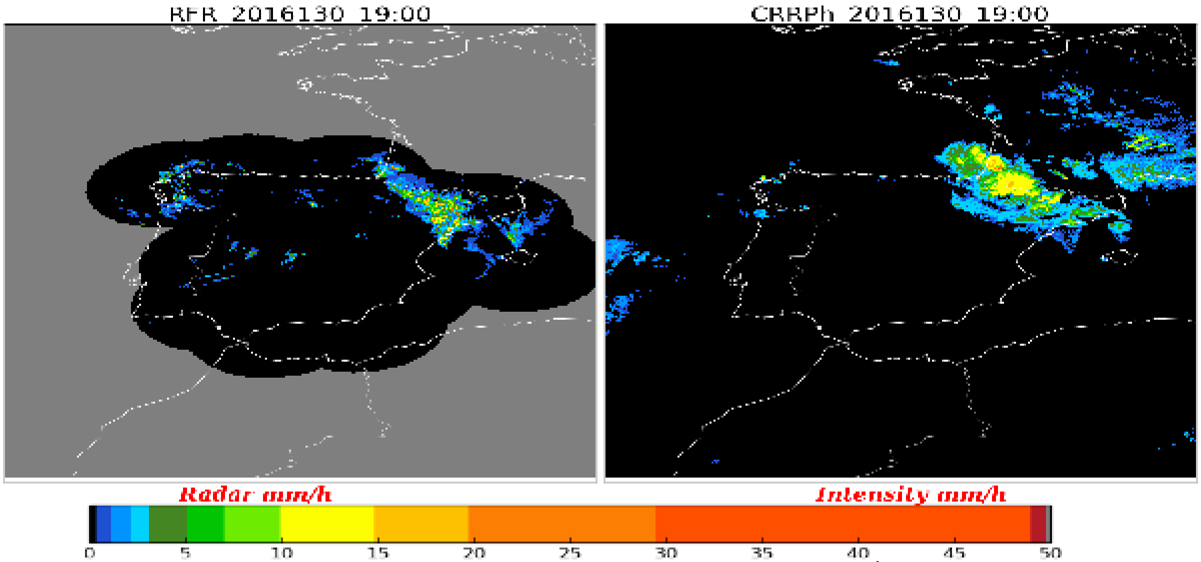

Figure 51. Comparison of radar (PPI) and CRR-Ph night product on 9th May 2016 at 23:00UTC

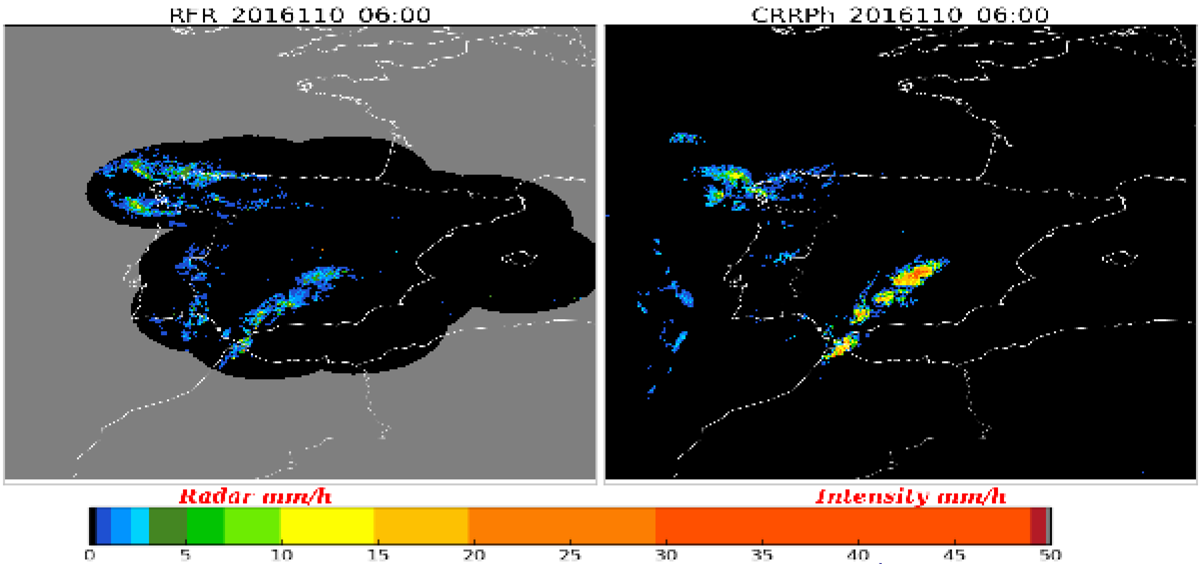

Figure 52. Comparison of radar (PPI) and CRR-Ph night product on 19th April 2016 at 23:00UTC

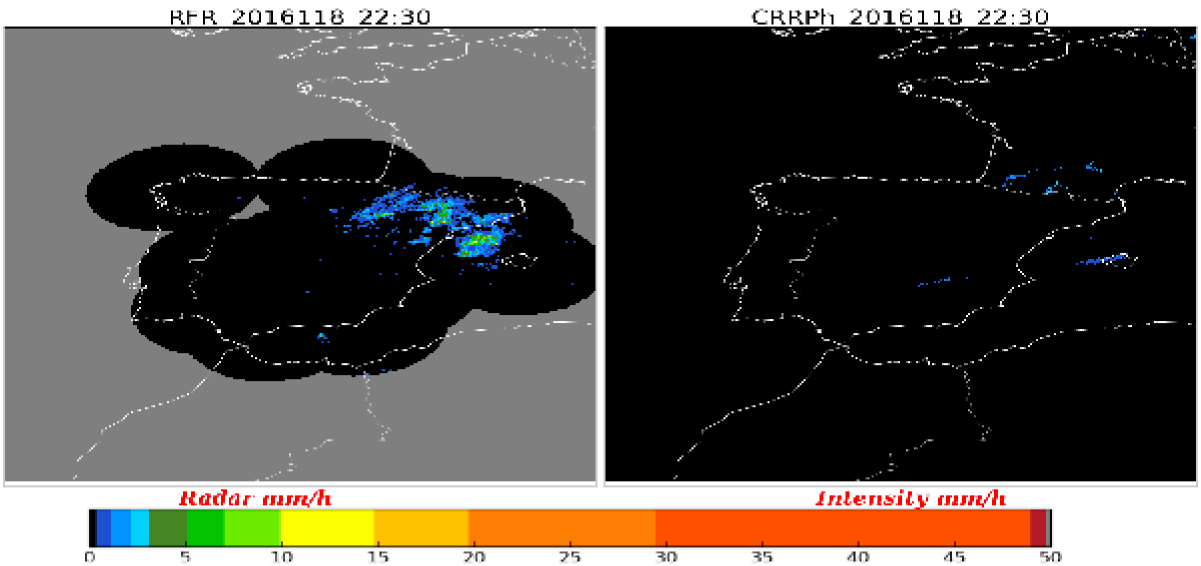

Figure 53. Comparison of radar (PPI) and CRR-Ph night product on 27th April 2016 at 22:30UTC

There have been plotted some examples where the CRR-Ph has had worse behaviour.
The CRR-Ph night product has two weak points. The first one lays on the fact that on some rain episodes it doesn´t detect the rain, an example of this situation is illustrated on figure 53. Rainy pixels over the north eastern region of Spain aren´t depicted by the product. This is not a very common behaviour but it is important to be mentioned.
In other circumstances the rainy area is well represented but the intensity not, having a rain rate overestimation. Pay attention to the convective areas over the middle and south of Spain, see figure 52.
Finally, on Figure 51, it appears over the northern region of Spain an extension of cold cirrus associated with a storm that makes the product overestimate the precipitating area.

5.2 Objective validation for Convective Rainfall rate from Cloud Physical Properties (CRR-Ph)

5.2.1 Validation Procedure

In this section an objective categorical validation has been conducted. POD and FAR indicators included in the "NWCSAF Product Requirements Document" [AD 4] have been evaluated. Instantaneous rain rates validation has been done against instantaneous rates taken from the Spanish radar PPI data.

Every slot has been classified as day slot, night slot or mixed, depending on the number of day or night pixels of each image. In order to evaluate the day algorithm separately from the night algorithm, mixed slots have been discarded. This way a day or night slot only contains pixels of the same category.

As far as the hourly accumulations is concerned, the validation has been done against the radar hourly accumulations, obtained from the 500m Pseudo-CAPPI. In this case a day-night distinction has also be taken into account, validating only pixels of the same category.

The CRR-Ph product has been calibrated with a list of days throughout 2015 that accomplished at least one of two criteria. Another list of days has been created throughout 2016, with the same criteria as 2015, to validate the product.

RFR in mm/h is obtained from the lowest Plan Position Indicator (PPI) of the radar using the Marshal-Palmer relation, $Z=200R^{1.6}$, where Z ($mm^6\ mm^{-3}$) is the reflectivity factor and R($mm\ h^{-1}$) is the rainfall rate. Echotop values in km. correspond with the maximum height that echoes bigger than 12dBz are able to reach.

First criterion: A particular day is included in the calibration and validation list if the percentage of pixels with ET>6km. with respects to pixels with ET>0 km exceeds the threshold of 65% at least for one slot of this day.

Second criterion: It is calculated the proportion of radar pixels with RFR>=0.2mm/h with respect to the whole image. Whenever at least one slot of a day reaches the percentage limit of 8% the day was also included in the calibration and validation list.

Since Microphysical Cloud Top parameters used by the CRR-Ph algorithm have been computed only for sun zenith angles lower than 70º, this validation has been undertaken under the same condition.

Since R_{eff} and COT parameters are not computed by CMIC for undefined Phase pixels, those cases have been excluded from validation.

Radar data, which are in Lambert Projection with a 1km*1km pixel resolution, have been converted into the MSG projection, using a bi-linear interpolation. The horizontal resolution of the MSG pixels are 3kms at satellite point. Parallax correction has been applied to the CRR-Ph product. As a perfect matching between Radar and MSG images is not possible, a smoothing process in 3x3 boxes pixels has been done.

A radar quality image has been used as a filter image to get rid of spurious echoes, such as windmill echoes. Anomalous propagation echoes have been removed through the 10.8IR scene. A rain image has been obtained from the 10.8IR data using the basic AUTOESTIMATOR algorithm (Vicente et al., 1998). A pixel with significant radar echo is considered to be a ground echo and set to zero if no significant value is found in a 15x15 box centred in the AUTOESTIMATOR image.

Despite the fact the product has been calibrated only in convective situations, it has been also generated in non-convective situations. For this reason it has been done a double validation: one in convective pixels, and the second one in all pixels. While the convective validation has been put into practise, a criterion to select convective areas is also necessary. The criteria consist of selecting those areas with ET>=6km, RFR>=3mm/h and a box size=15*15 pixels. There is a little bit of arbitrariness behind this election, because other selections are also possible.

Before calculating the POD and FAR scores, correct negatives (see Table 30 in ANNEX 1: VERIFICATION METRIC section) have been filtered because they represent a big number of the data population, reduce speed computing and they are not involved in the categorical scores formula.

Due to the temporal resolution of the SEVIRI data in the normal mode, there are four CRR-Ph outputs available every hour. The Spanish radar network generates a set of instantaneous products every 10 minutes. The MSG scanning over Spain is done over 10 minutes after the slot hour. The only way to temporally match CRR-Ph product with radar images is choosing 0 and 30 minutes CRR-Ph images corresponding to 10 and 40 minutes radar images respectively. This way 15 and 45 minutes CRR-Ph images, which don't temporally match with the radar images, haven't been used in the validation process.

Both categorical and accuracy statistic have been used to validate the product. They are explained in ANNEX 1: VERIFICATION METRIC.

5.2.2 Instantaneous Rain Rates

5.2.2.1 CATEGORICAL VALIDATION

In order to compute the categorical scores, two thresholds have been stablished, one for the CRR-Ph and another one for the rainy pixels of the radar.
The CRR-Ph threshold for an instantaneous rain rate is fixed to 0.2 mm/h or higher.
The rainy pixels from the radar are fixed to at least 0.2 mm/h.

5.2.2.1.1 DAY

5.2.2.1.1.1 Convective Areas

N	POD (%)	FAR (%)	CSI (%)	PC (%)
1160269	74.24	**35.05**	53.00	53.00

Table 22. Categorical scores for CRR-Ph day algorithm in convective areas

5.2.2.1.1.2 All Areas

N	POD (%)	FAR (%)	CSI (%)	PC (%)
4208125	57.89	49.66	36.85	36.85

Table 23. Categorical scores for CRR-Ph day algorithm in all areas

5.2.2.1.2 NIGHT

5.2.2.1.2.1 Convective Areas

N	POD (%)	FAR (%)	CSI (%)	PC (%)
3397658	42.29	**36.42**	34.05	34.05

Table 24. Categorical scores for CRR-Ph night algorithm in convective areas

5.2.2.1.2.2 All Areas

N	POD (%)	FAR (%)	CSI (%)	PC (%)
15403702	26.90	67.44	17.27	17.27

Table 25. Categorical scores for CRR-Ph night algorithm in all areas

Hourly Accumulations

With the aim of computing the categorical scores for the hourly accumulations, two thresholds have been stablished, one for the CRR-Ph and another one for the rainy pixels of the radar.
The CRR-Ph threshold is fixed to 0.2 mm/h or higher.
The rainy pixels from the radar are fixed to at least 0.2 mm/h.

As it can be noticed it has been established a discrimination between convective and non-convective areas. Those convective areas have been selected taking into account that the convective area must keep active during one hour, which involves three different slots, the current one and two preceding.

Having stablished the difference between convective and non-convective areas, the improvement in the categorical scores in convective areas becomes evident in comparison with all areas. This way, POD and FAR scores are fulfilled for both, day and night, in convective areas.

5.2.2.2 DAY

N	POD (%)	FAR (%)	CSI (%)	PC (%)
265782	**82.35**	**12.10**	73.97	73.97

Table 26. Categorical scores for CRR-Ph day algorithm in convective areas

N	POD (%)	FAR (%)	CSI (%)	PC (%)
2198129	61.92	39.52	44.08	44.08

Table 27. Categorical scores for CRR-Ph day algorithm in all areas

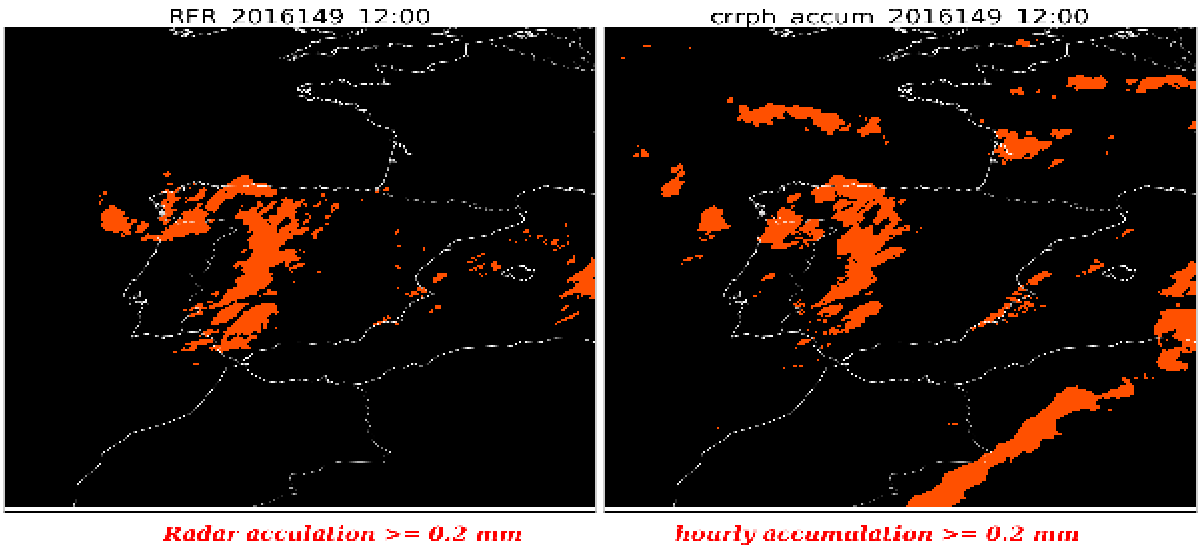

Figure 54. Comparison of one hour radar accumulation and CRR-Ph hourly accumulation day product on 28th May 2016 at 12:00UTC

We should not pay attention to those areas depicted in crrph_accum out of Spain radar coverage.

5.2.2.3 NIGHT

N	POD (%)	FAR (%)	CSI (%)	PC (%)
885197	**52.84**	**14.35**	48.54	48.54

Table 28. Categorical scores for CRR-Ph night algorithm in convective areas

N	POD (%)	FAR (%)	CSI (%)	PC (%)
8815013	28.67	63.24	19.20	19.20

Table 29. Categorical scores for CRR-Ph night algorithm in all areas

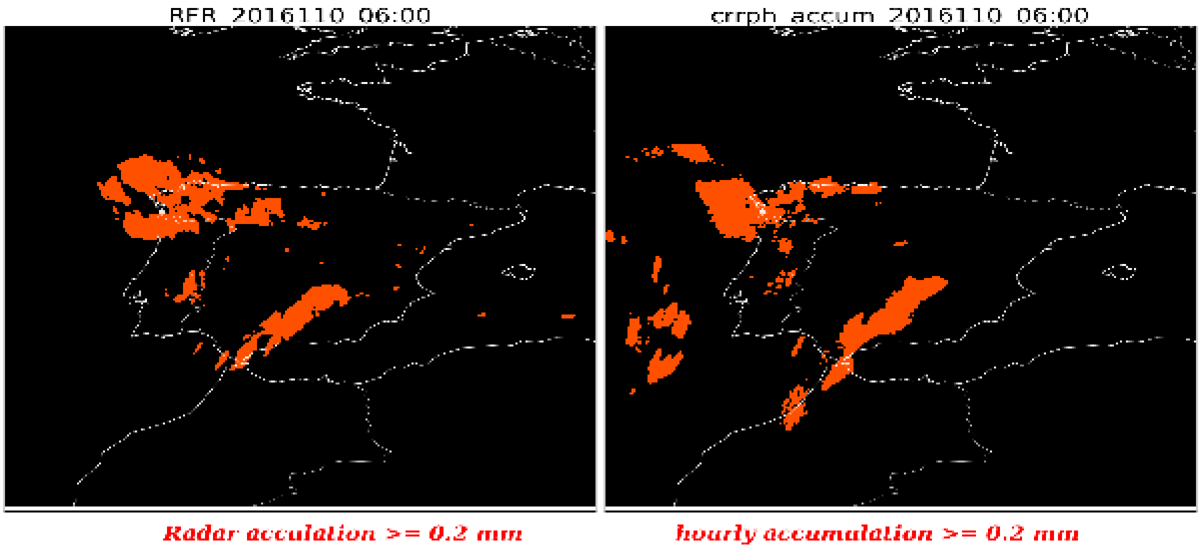

Figure 55. Comparison of one hour radar accumulation and CRR-Ph hourly accumulation night product on 19th April 2016 at 12:00UTC

5.2.3 Conclusions

With respects to the instantaneous rain rates, POD and FAR scores are better in convective areas than in all areas and results are also better during day time than during night time.

Despite a general good behaviour of the CRR-Ph day product in convective areas there isn't a perfect spatial matching between radar pixels and the CRR-Ph product. A spatial displacement between radar pixels and CRR-Ph pixels penalizes the product. It is known that in an objective validation made pixel by pixel, collocation problems between radar and satellite makes the double penalty problem visible.

According to the "NWCSAF Product Requirements Document" [AD 4], POD score corresponding to the CRR-Ph instantaneous rate during day time on convective areas is truly close to be achieved (it is missing less than a point). However, POD score doesn´t reach the target at night but is approaching to it. FAR score is fulfilled. (Green bold colour is chosen when stablished limits are fulfilled).

At night there are some episodes of rain that are invisible to the CRR-Ph night product. Low top precipitating clouds with warn tops are not well distinguished. There are other situations where it happens just the opposite. There is an overestimation of the rain area due the cold cirrus extension at high levels associated with developed convective clouds.

Regarding the CRR-Ph hourly accumulation, it inherits the same strong and weak points from its precursor CRR-Ph instantaneous rain rate. Better results are obtained at day time than night time and also are better in convective areas compared with all areas.

At day time POD and FAR requirements are both fulfilled, however it doesn't happen the same at night time.

6. HIMAWARI DATA

Both PC-Ph and CRR-Ph products have been computed taken Himawari-8 satellite data as a new input. The remaining inputs, CMIC and NWP models have been computed changing the area of study (Asia region). In order to have a visual validation, a Japanese radar reflectivity composite imagery have been depicted obtained from the NCAR/EOL (website: https://www.eol.ucar.edu/data software) data archive. Three different days at 00Z are shown below. The images chosen include both day and night algorithm. Day-night line division can be noticed at west part of North Korea.

Taken a look to the different pictures depicted below, it can be noticed a general good performance of both the PC-Ph and the CRR-Ph products. The precipitating structures detected by the radar keep the same appearance in both products. It has been taken into account that the radar imagery are represented in a different projection from the precipitation products. It is important to keep in mind that the PC-Ph and the CRR-Ph product have been calibrated with another satellite input (MSG), despite this aspect it has a general good behaviour. It seems that the same strong and weak points commented in previous sections persist and are visible for Himawari-8. The PC-Ph product tends to overestimate the precipitation area and hardly reach probabilities of 80% or higher. With respect to the CRR-Ph it reproduces the same radar precipitating patterns with a slight overestimation in some areas. It has not been forgotten that the CRR-Ph has been calibrated in convective areas and in this cases of study we haven´t distinguished between convective or non-convective areas.

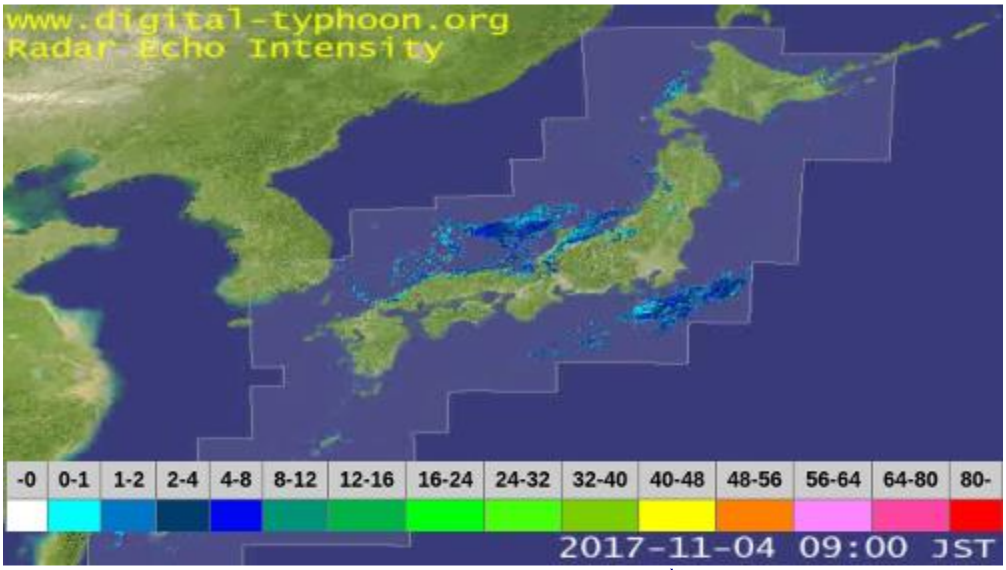

Figure 56. Composite weather radar echoes (mm/h) on 4th November 2017 at 00:00 UTC

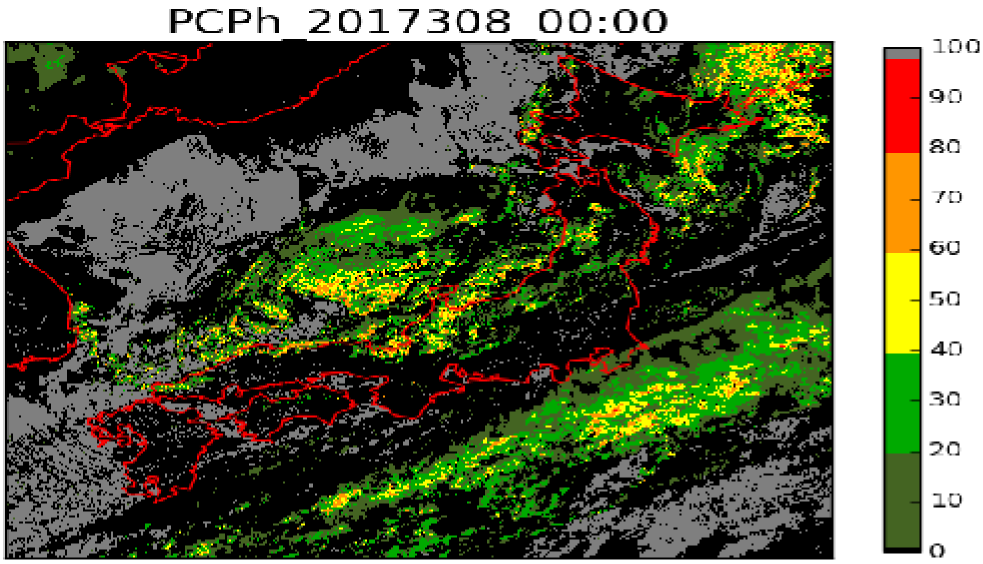

Figure 57. PC-Ph product on 4th November 2017 at 00:00 UTC

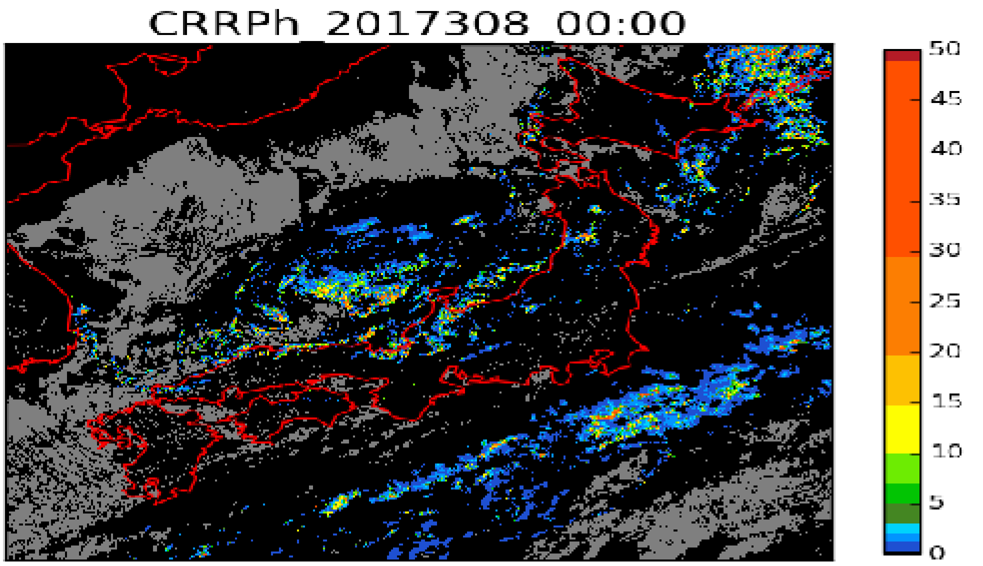

Figure 58.CRR-Ph product on 4th November 2017 at 00:00 UTC

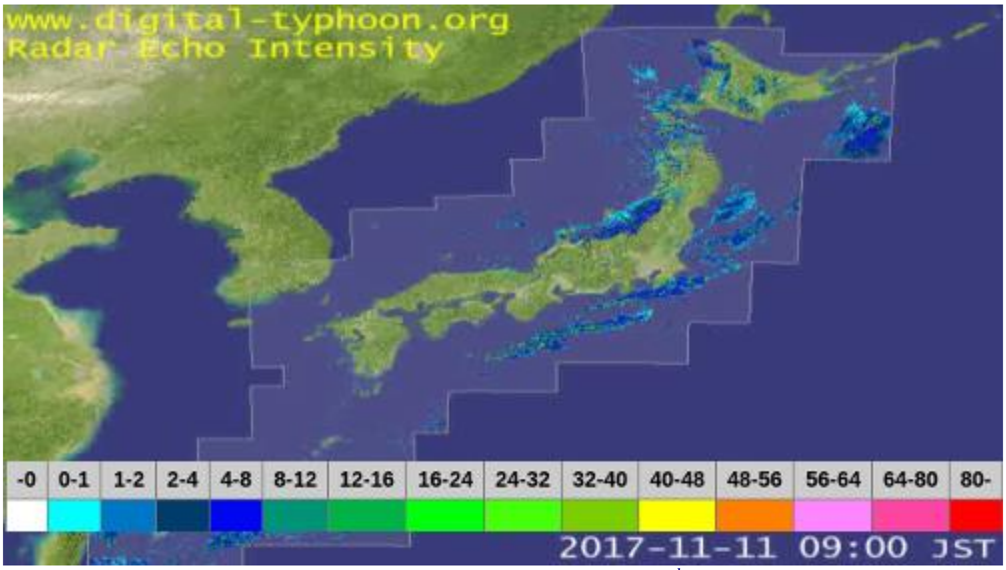

Figure 59. Composite weather radar echoes (mm/h) on 11th November 2017 at 00:00 UTC

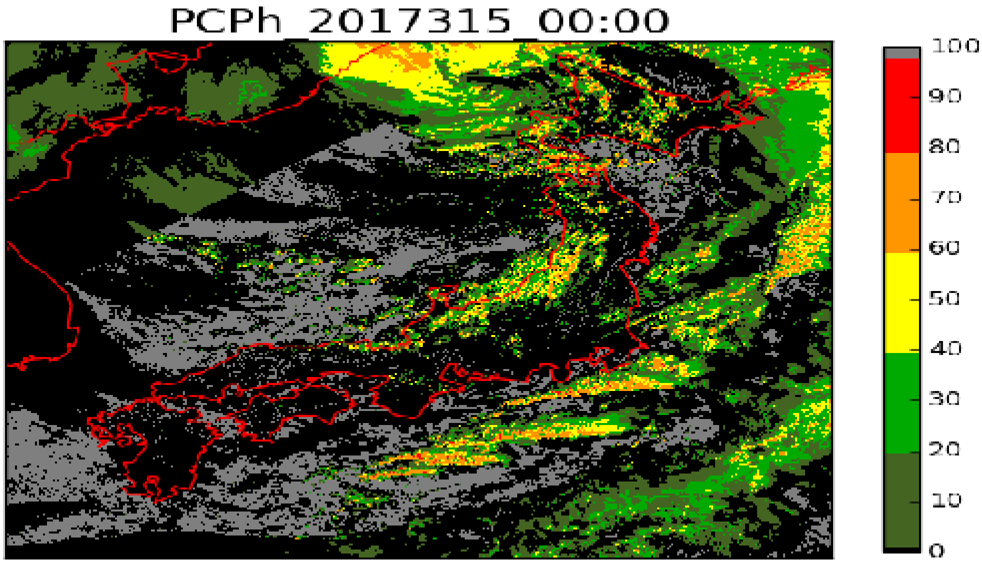

Figure 60. PC-Ph product on 11th November 2017 at 00:00 UTC

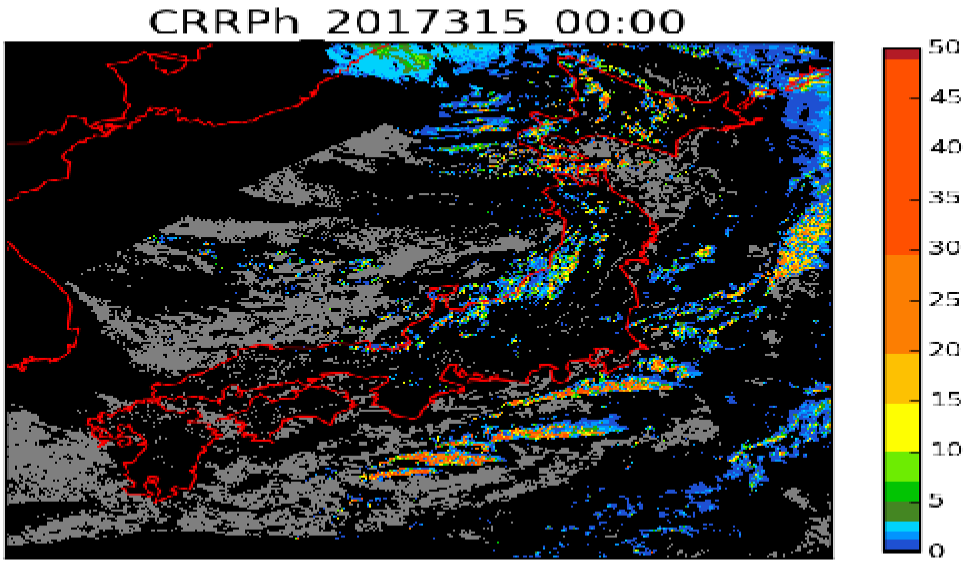

Figure 61. CRR-Ph product on 11th November 2017 at 00:00 UTC

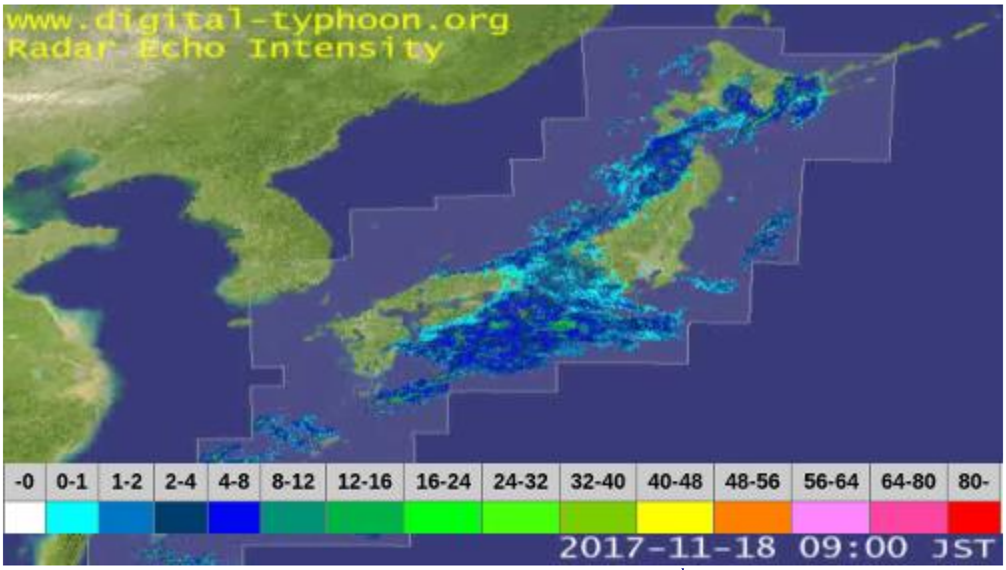

Figure 62. Composite weather radar echoes (mm/h) on 18th November 2017 at 00:00UTC

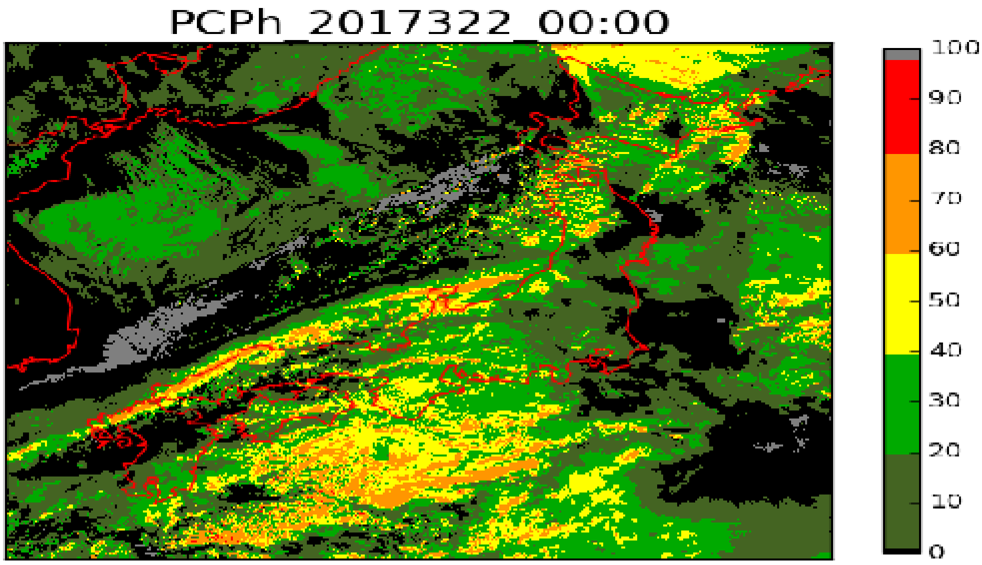

Figure 63. PC-Ph product on 18th November 2017 at 00:00UTC

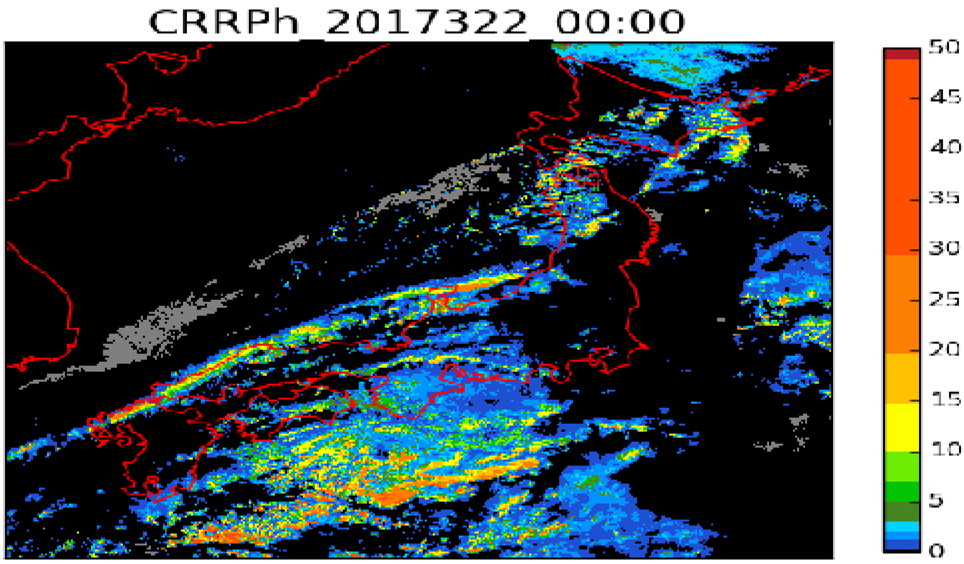

Figure 64. CRR-Ph product on 18th November 2017 at 00:00 UTC

7. GOES-16 DATA

CRR , PC-Ph and CRR-Ph have been generated over North America. A composite imagery of radar data is available on the following website: https://gis.ncdc.noaa.gov/maps/ncei/radar .
A visual validation between the precipitating products and the radar data (in dBz) have been done.
GOES-16 satellite data, NWP models, CMIC and Cloud products have been necessary to compute the precipitating products.

Two days have been selected: 2th May 2018 and the 6th July 2018 at 23:45Z and 00:00Z respectively. This time slots allow us to visualize both day and night algorithms at the same time. Night algorithm is on the right site of the image and day algorithm on the left site. Transition between both algorithms is recognizable by a line that goes from north to south. On Figure 67 the transition becomes evident focusing on the left of Nebraska, Dodge and Abilene.

To have a more detailed information, a zoom up have been done the 6th July 2018 00:00Z time slot. The geographical coordinates of the lower-left corner and the upper-right corner in degrees are: (lon = -111.594 , lat = 33.70) and (lon = -96.004, lat = 41.056). In this case the zoom up region matches with the day algorithm.

In general, it shows a good behaviour of the three products, being more accurate the day algorithm and also the CRR-Ph with respects to the CRR.

As it has been commented before, it should be taken into account that all the precipitating products have been calibrated in convective areas over Europe. Beside this aspect it reproduces quite well the rain patterns. It seems that the same strong and weak points commented in previous sections persist and are visible for GOES-16. The PC-Ph tend to slighly overestimate the precipitating regions and hardly reach probabilities higher than 80%. The CRR-Ph has a quite similar shape with respects to the radar echoes but it does not always place the same intensity than the radar does.

7.1 2TH MAY 2018

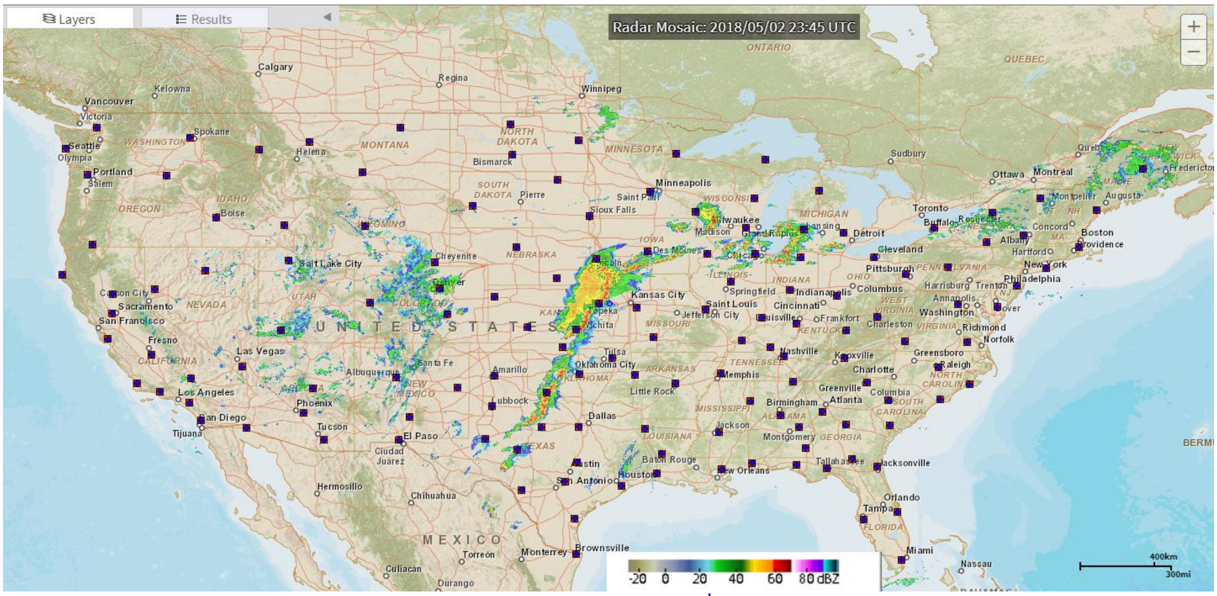

Figure 65. USA Radar mosaic (dBz) on 2th May 2018 at 23:45 UTC

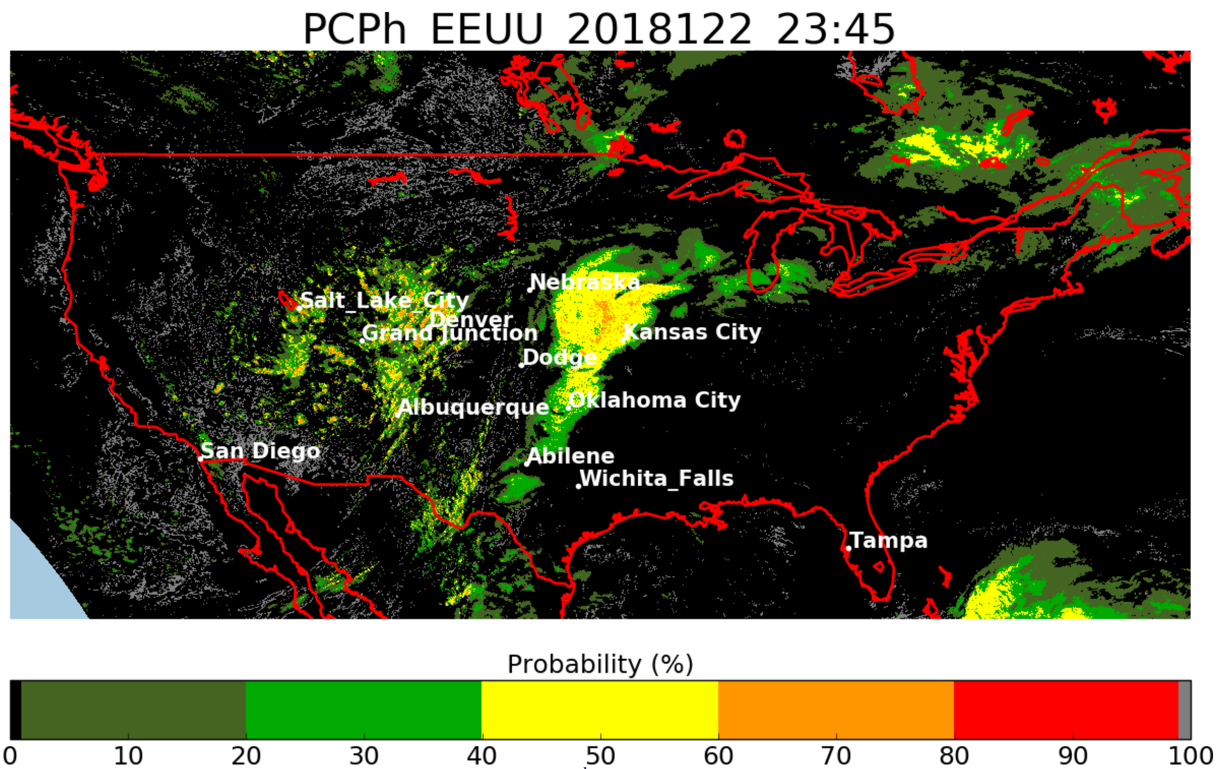

Figure 66. PC-Ph product on 2th May 2018 at 23:45 UTC over USA.

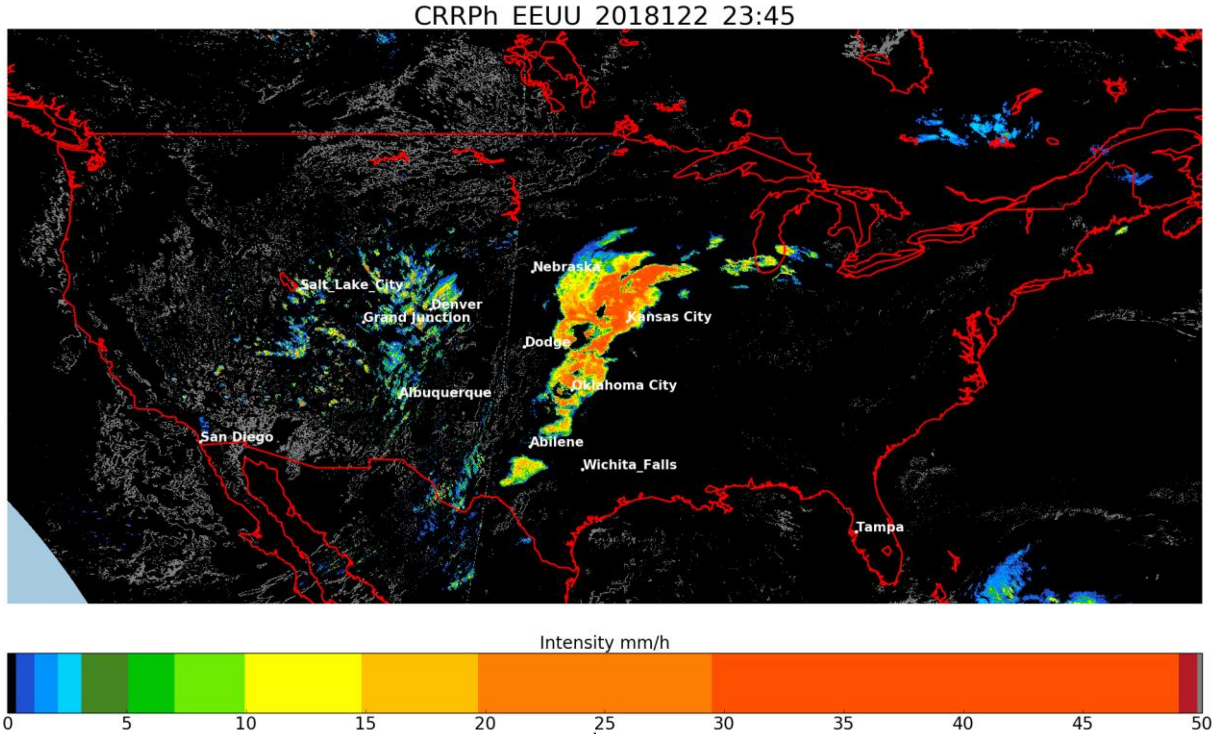

Figure 67. CRR-Ph product on 2th May 2018 at 23:45 UTC over USA.

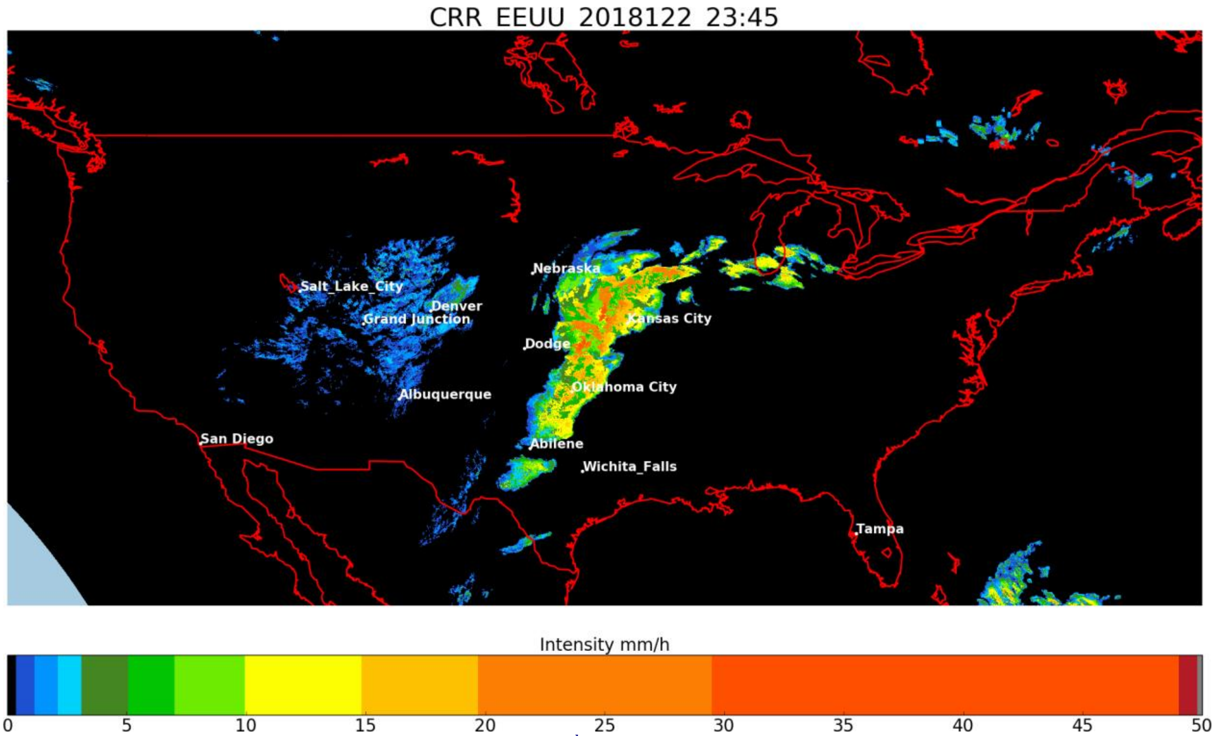

Figure 68. CRR product on 2th May 2018 at 23:45 UTC over USA.

7.2 6TH JULY 2018

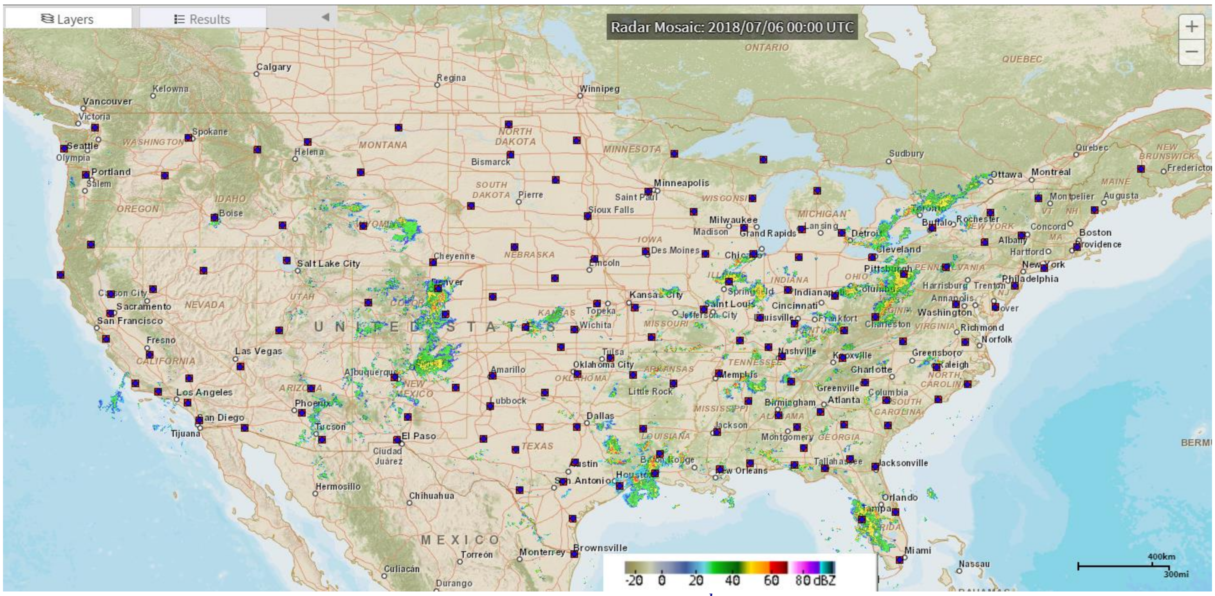

Figure 69. USA Radar mosaic (dBz) on 6th July 2018 at 00:00 UTC

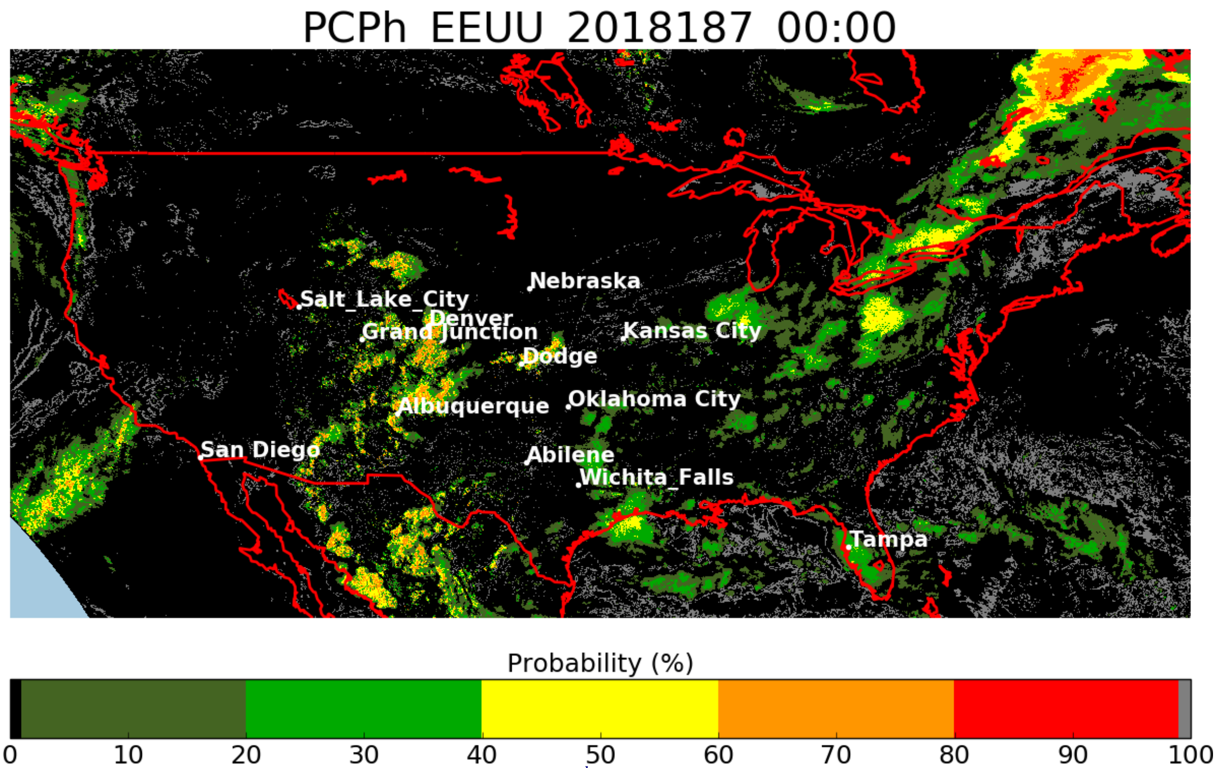

Figure 70. PC-Ph product on 6th July 2018 at 00:00 UTC over USA.

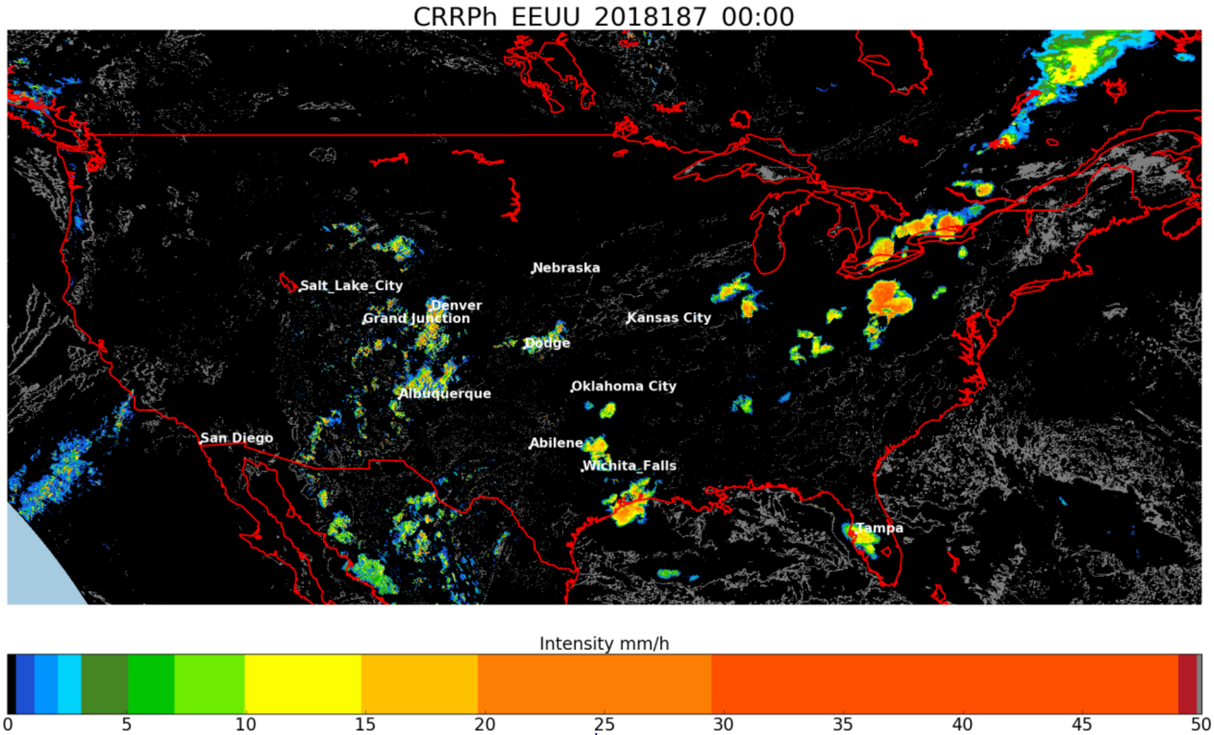

Figure 71. CRR-Ph product on 6th July 2018 at 00:00 UTC over USA.

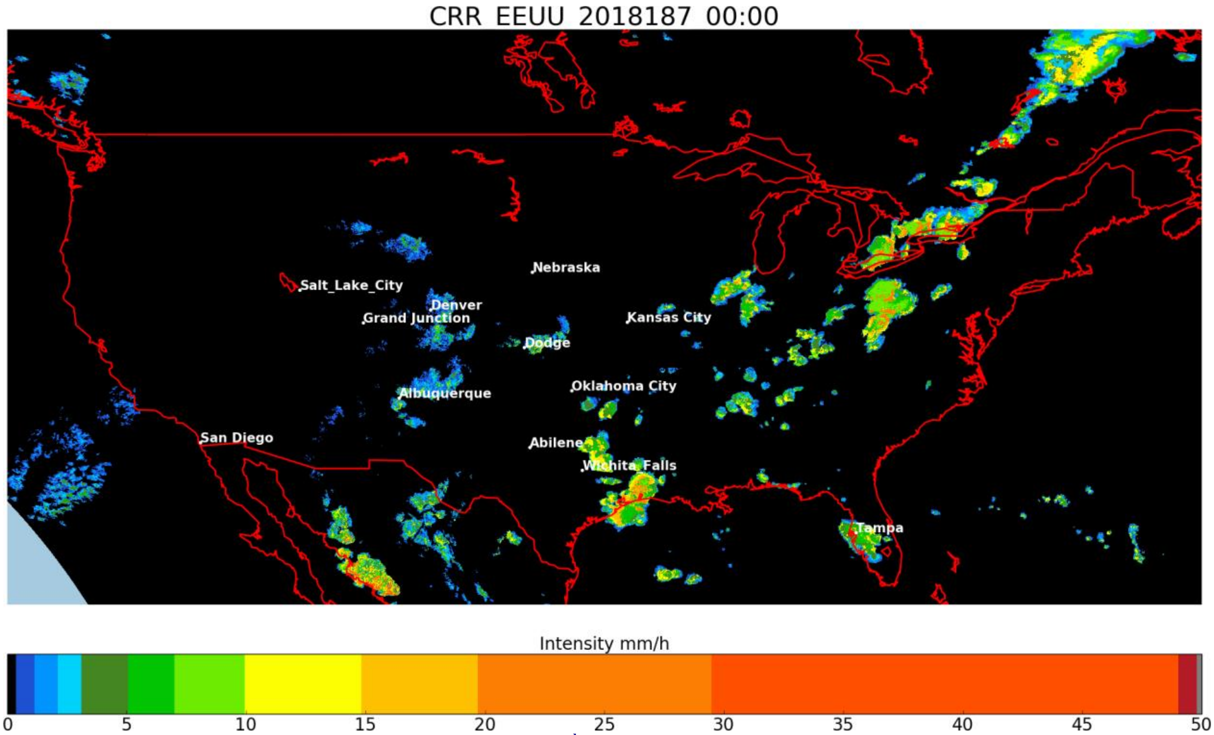

Figure 72. CRR product on 6th July 2018 at 00:00 UTC over USA.

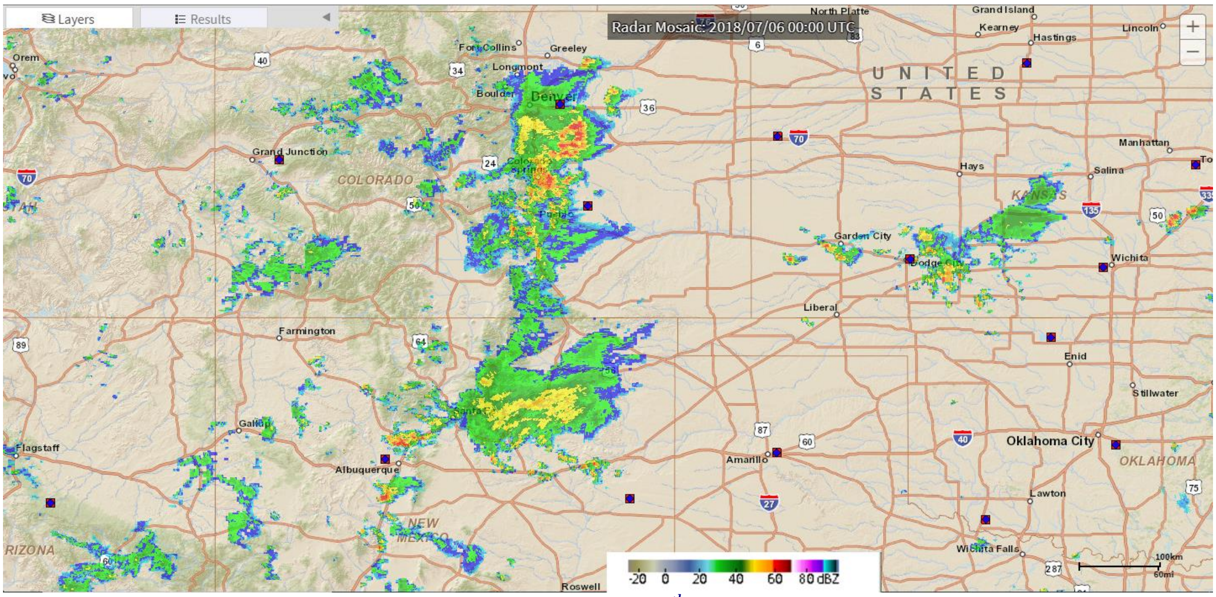

Figure 73. Radar mosaic (dBz) on 6th July 2018 at 00:00 UTC.

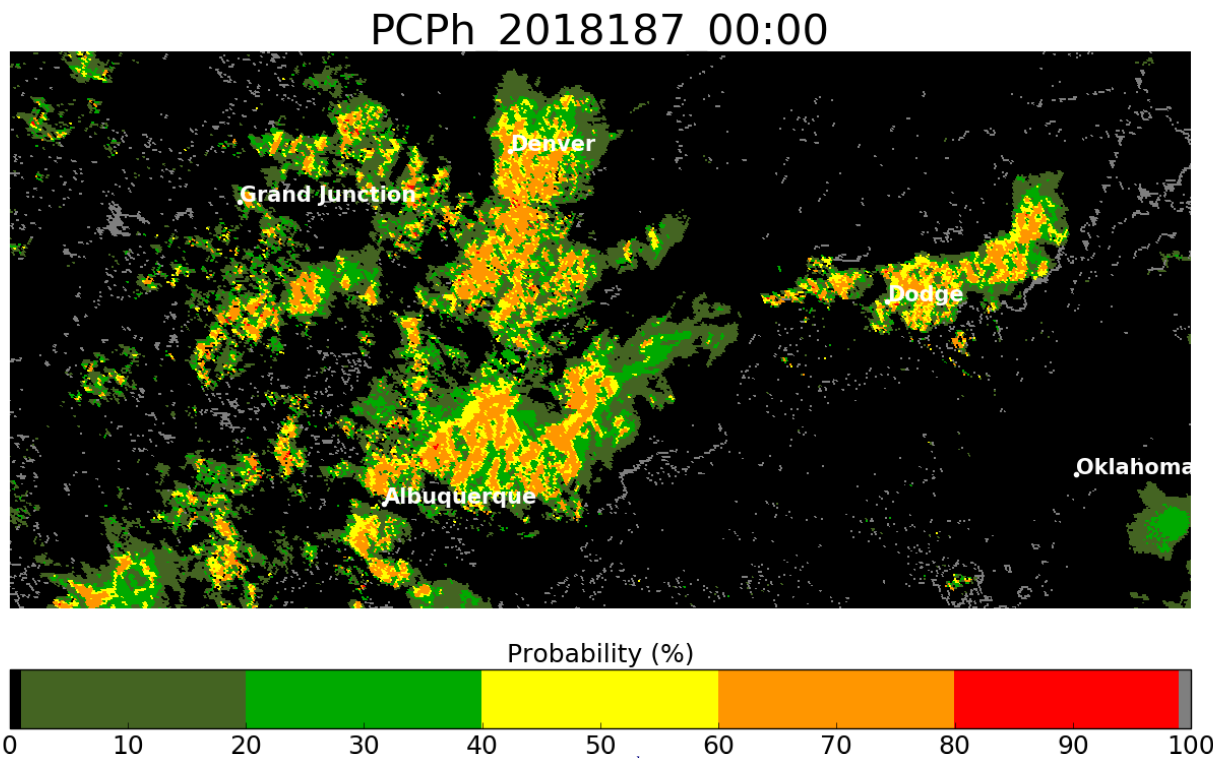

Figure 74. PCPh product on 6th July 2018 at 00:00 UTC..

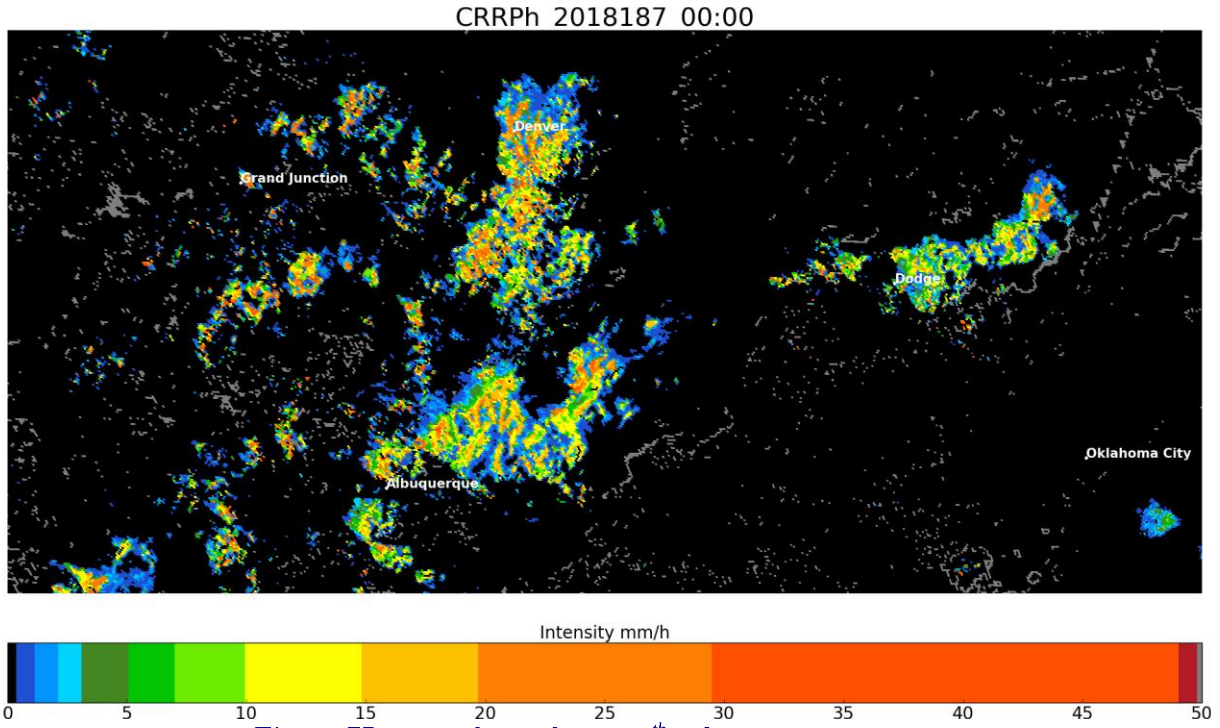

Figure 75. CRR-Ph product on 6th July 2018 at 00:00 UTC.

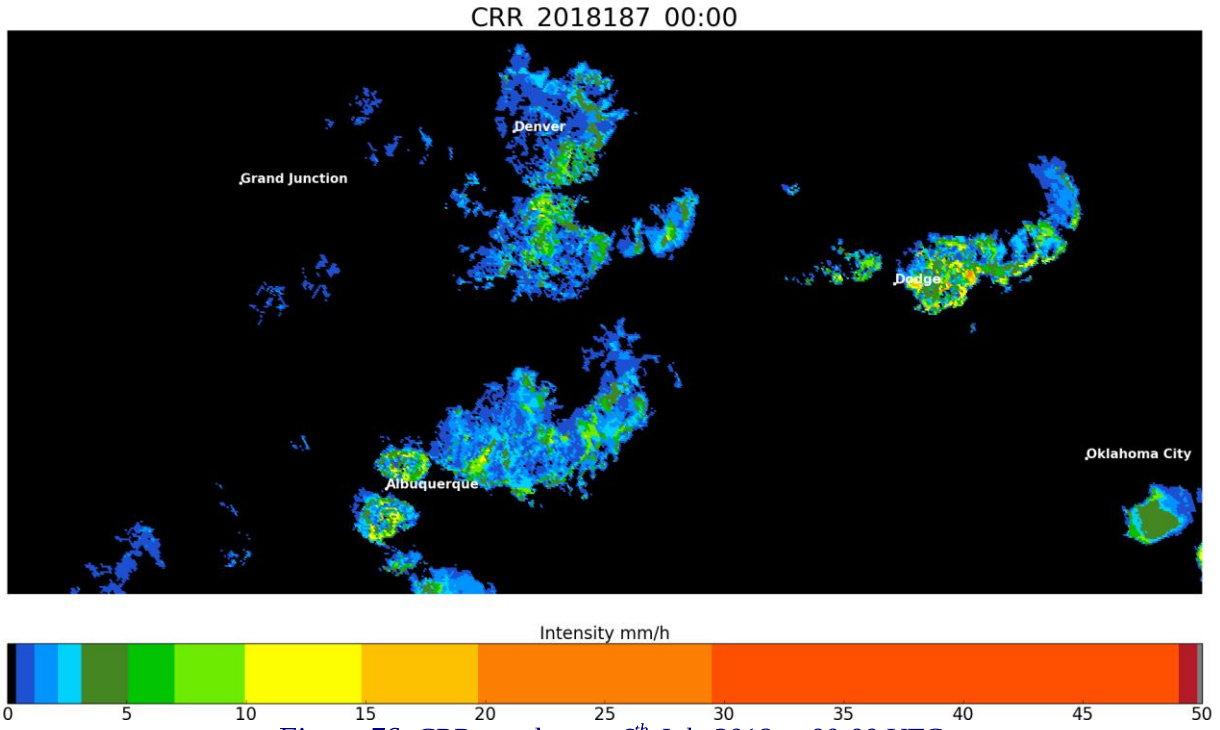

Figure 76. CRR product on 6th July 2018 at 00:00 UTC

8. ANNEX 1: VERIFICATION METRIC

CATEGORICAL STATISTICS

The following scores derived from Table 30, have been calculated:

- False Alarm Ratio:

$$FAR = \frac{false\_alarms}{hits + false\_alarms}$$

Measures the fraction of estimated events that were actually not events.

- Probability of Detection:

$$POD = \frac{hits}{hits + misses}$$

Measures the fraction of observed events that were correctly estimated.

- Critical Success Index:

$$CSI = \frac{hits}{hits + misses + false\_alarms}$$

Measures the fraction of observed and/or estimated events that were correctly diagnosed.

- Percentage of Corrects:

$$PC = \frac{hits + correct\_negatives}{hits + misses + false\_alarms + correct\_negatives}$$

Is the percentage of correct estimations.

		Estimated (CRR-Ph,PC-Ph)	
		occurred[1]	no occurred
Observed (Radar)	occurred*	hits	misses
	no occurred	false alarms	correct negatives

Table 30. Contingency table convention

9. REFERENCES

Vicente, G.A., Scofield, R.A. and Menzel W.P. 1998: The Operational GOES Infrared Rainfall Estimation Technique, Bull. American Meteorological Society, Vol. 79, No. 9, pp. 1883-1898.

[1] *Occurred means values higher than or equal to 0.2 mm/h for instantaneous rates and higher than or equal to 0.2 mm for hourly and daily accumulations.*